A

B

C

FIG. 2. Role of an HCV core protein NLS in nuclear localization of JEV core protein. (A) A partial alignment of amino acid sequences of core proteins of HCV (HCVJ1 strain, genotype 1b) and flaviviruses, including JEV, SLE (St. Louis encephalitis virus), KUN, WNV, MVE (Murray Valley encephalitis virus), and DENs. Amino acid sequences of the HCV core protein and identical amino acids in flaviviruses are indicated with red letters. Amino acids that were completely conserved among the viruses are indicated by asterisks and red boldface letters. The NLS of HCV core protein previously reported by Suzuki et al. (54) is underlined. (B) Expression plasmids encoding EGFP-fused JEV core proteins mutated in the NLS of the HCV core protein. The presence (+) or absence (−) of nuclear localizations of the EGFP-fused JEV core proteins is indicated. Dots indicate the deleted amino acids. Boldface letters indicate the substituted amino acids. (C) Intracellular localization of EGFP-fused JEV core proteins with deletion or substitution in the NLS region of HCV core protein in Vero cells. Panels (except for panel f) indicate merged images of EGFP and nuclear staining by propidium iodide. Panel f shows merged images of EGFP-fused JEV core protein with a G^{42}-to-Ala substitution and a major nucleolar protein nucleolin. All samples were observed with a confocal microscope.

these flaviviruses and HCV. Therefore, we next analyzed the effect of mutation in this region on the nuclear localization of the JEV core protein. The EGFP-fused JEV core protein with residues 39 to 44 deleted was localized only in the cytoplasm but not in the nucleus (Fig. 2B and panel a in Fig. 2C). To further identify the essential amino acids for the nuclear localization, a series of point mutants were constructed (Fig. 2B). No single-amino-acid substitution of the core proteins abolished nuclear localization except for a mutant of Gly^{42} in which the mutant core protein did not colocalize with nucleolin and was distributed as filamentous structures in the nuclei (Fig. 2C, panels e and f). However, double substitutions of the most conserved Gly^{42} and Pro^{43} to Ala completely eliminated the nuclear localization of the JEV core protein (Fig. 2C, panel i). These results indicate that Gly^{42} and Pro^{43}, which are well conserved among flaviviruses and HCV (Fig. 2A), are important for nuclear and nucleolar localization of the JEV core protein.

Mutant JEV lacking the nuclear localization of core protein. To generate a mutant JEV incapable of localizing the core protein in the nucleus, synthetic RNA transcribed from pMWJEAT/GP4243AA encoding a full-length cDNA of mutant JEV M4243 under the T7 promoter was electroporated into Vero cells. The wild type, which was similarly generated from pMWJEATG1, and M4243 viruses were amplified in C6/36 cells after recovery from Vero cells because of a low viral yield of M4243 virus in Vero cells after electroporation (2×10^3 FFU/ml at 3 days after transfection) and used in subsequent experiments. The entire genomic cDNAs of the recovered viruses were confirmed to be identical to those of the infectious clones by direct sequencing. Intracellular localization of core proteins of the wild-type and mutant JEVs was examined in Vero and C6/36 cells by an immunofluorescence assay. In both cell lines, the core protein of the wild-type virus was localized in both the cytoplasm and nuclei whereas the core protein of M4243 was detected only in the cytoplasm and not in nuclei in both cell lines, as we expected (Fig. 3A). To confirm the intracellular localization of the core proteins, cytoplasmic and nuclear fractions of Vero cells infected with the viruses were analyzed by Western blotting (Fig. 3B). The wild-type core protein was fractionated in both cytoplasmic and nuclear fractions, while the mutant core protein was detected in the cytoplasmic fraction but not in the nuclear fraction.

Growth properties of the mutant JEV in vitro. To examine the roles of the nuclear localization of the core protein in viral propagation, one-step growth kinetics of the viruses in Vero and C6/36 cells were determined after inoculation at an MOI of 5 (Fig. 4A). The M4243 virus exhibited impaired propagations, with the infectious titers being 773- and 31-fold lower than those of wild-type JEV at 30 h postinoculation in Vero and C6/36 cells, respectively. These results indicate that Gly^{42} and Pro^{43} in the JEV core protein were important for viral propagation, especially in Vero cells. The size of infectious foci in Vero cells produced by the M4243 virus recovered from the culture supernatants at 1 day postinfection of Vero cells was markedly smaller than that of the wild-type virus (Fig. 4B, left and middle panels). However, supernatants of Vero cells recovered 3 days after infection with M4243 produced larger foci than those obtained after incubation for 1 day (Fig. 4B, right panel). This phenomenon was not observed in C6/36 cells. To
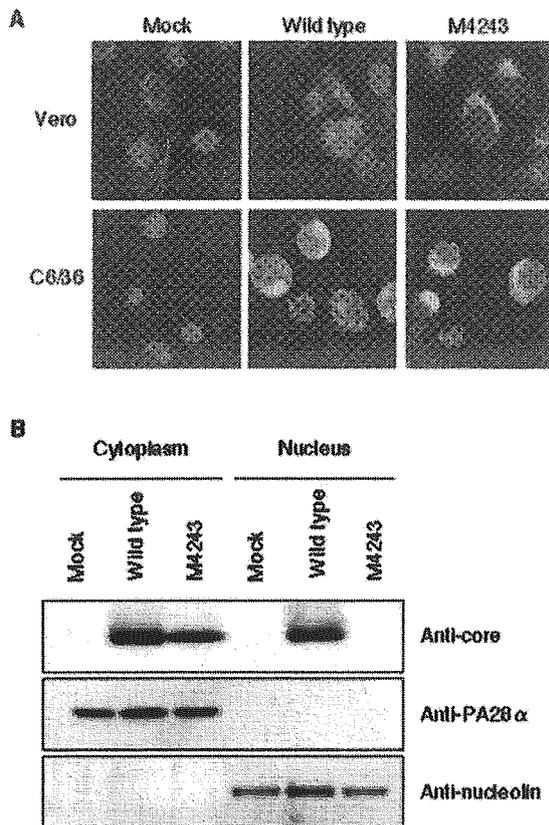
A

B

FIG. 3. Intracellular localization of core proteins in cells infected with wild-type or M4243 virus. (A) Intercellular localization of wild-type and mutant JEV. Vero or C6/36 cells were infected with wild-type or M4243 virus, fixed at 2 days postinoculation and immunostained with anti-JEV core rabbit serum. Nuclei were stained with propidium iodide. All samples were observed with a confocal microscope. (B) Intracellular fractionation of Vero cells infected with the viruses. The core proteins in the cytoplasmic and nuclear fractions were detected by Western blotting with the anti-JEV core rabbit serum. Endogenous proteins PA28α and nucleolin were detected as controls for the cytoplasmic and nuclear fractions, respectively.

assess the possibility of the emergence of revertant viruses, the nucleotide sequences of two independent clones obtained at 3 days postinfection with M4243 in Vero cells were determined by direct sequencing. The majority of viruses carried a single-amino-acid reversion from Ala to Gly (GCG to GGG) at residue 42 in both clones. The single mutation of Pro[43] to Ala of the EGFP-fused JEV core protein did not abolish the nuclear or nucleolar localization, as shown in Fig. 2C (panel g). These results also support the idea that nuclear—especially nucleolar—localization of the JEV core protein is important for viral propagation in Vero cells.

Characterization of the released particles. It has been established that the flavivirus core protein is involved in the assembly and budding of infectious particles as a structural protein (34). Mutations in the core protein might posses the possibility to inhibit the release of infectious particles and, inversely, increase production of defective particles as described in previous reports (25, 26). Therefore, we determined the ratios between the infectivities and quantities of the par-
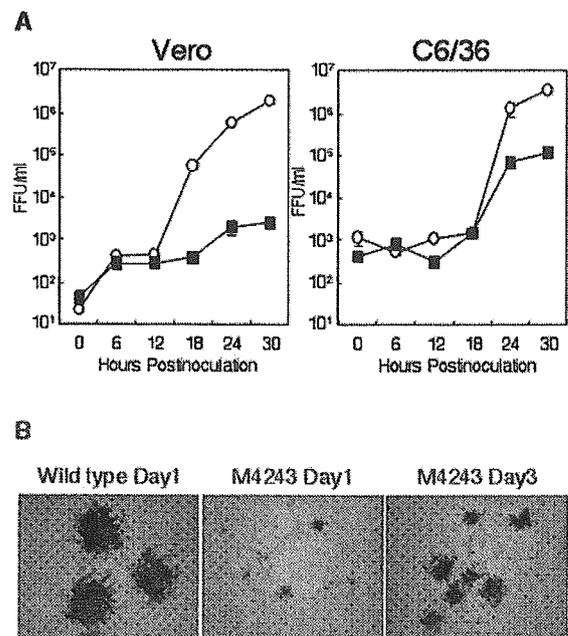
A

B

FIG. 4. Growth properties of wild-type and M4243 viruses. (A) Growth kinetics of the viruses in Vero and C6/36 cells. Both cell lines were infected with wild-type or M4243 virus at an MOI of 5. Culture supernatants were harvested at the indicated times postinoculation, and infectious titers were determined by focus-forming assays using Vero cells. Open circles and closed squares indicate the wild-type and M4243 viruses, respectively. Means of three experiments are indicated. (B) Infectious focus formation of the wild-type and M4243 viruses on Vero cells. Culture supernatants recovered at 1 or 3 days postinoculation in Vero cells were inoculated onto Vero cells and incubated for 3 days with methylcellulose overlay medium. The infectious foci were immunostained as described in Materials and Methods.

ticles released from Vero and C6/36 cells infected with the wild-type or M4243 JEV. The HA assay is able to detect viral particles irrespective of infectivity, because HA activity of the flavivirus is associated with E protein (28, 29). As shown in Table 1, the FFU/HA ratios of the wild-type JEV were significantly higher than those of the M4243 virus in both Vero and C6/36 cells, indicating that the M4243 virus produced a larger amount of defective particles than the wild-type virus. Although the ratios of defective particle production were equivalent between Vero and C6/36 cells, the mutant virus exhibited an HA titer comparable to that of the wild-type virus in C6/36 cells but significantly lower than that of the wild-type virus in Vero cells. In addition, the marked difference of infectious

TABLE 1. Infectious and HA titers of wild type and M4243 viruses derived from Vero and C6/36 cells

Cell	Virus[a]	FFU/ml	HA/ml	FFU/HA
Vero	Wild type	1.4×10^{10}	25600	5.5×10^5
	M4243	1.1×10^6	400	2.8×10^3
C6/36	Wild type	1.9×10^9	200	9.5×10^6
	M4243	4.0×10^7	800	5.0×10^4

[a] Viruses were 100-fold concentrated by a polyethylene glycol precipitation and determined the infectivities and HA activities.
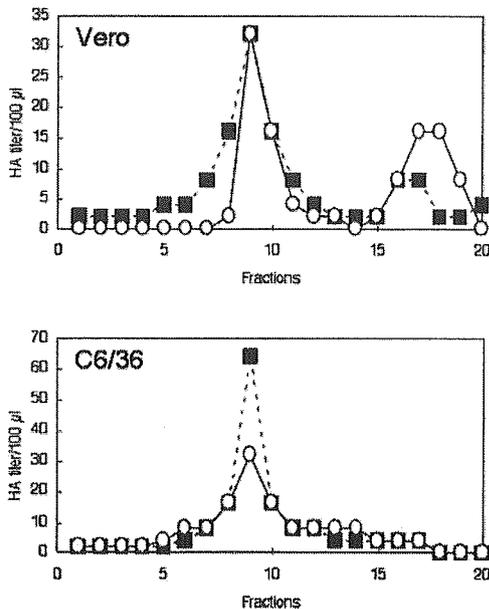
FIG. 5. Gradient fractionation of viral particles of the wild-type and M4243 viruses. The viral particles (400 HA units) derived from Vero or C6/36 cells were applied to 10 to 40% (wt/wt) sucrose gradient and centrifuged at 147,000 × g for 90 min. Twenty fractions were collected from bottom to top and quantified by the HA test. Open circles and closed squares indicate the wild-type and M4243 viruses, respectively. The representative data from three experiments are indicated.

titers between the wild-type and M4243 viruses in Vero cells (Fig. 4A) indicates that there may be another mechanism(s) underlying the low-growth properties of the M4243 virus in Vero cells besides the increased production of defective particles. To examine the production of subviral particles in culture supernatants of cells infected with M4243 virus, we carried out gradient fractionations and quantifications of viral particles by HA assay. As indicated in Fig. 5, the patterns of the fractionations of the particles of the M4243 virus were similar to those of the wild-type virus in both Vero and C6/36 cells, and subviral particles were detected in the fractions (fractions 16 to 19) of the supernatants of Vero cells infected with the wild-type or M4243 JEV.

Effect of nuclear localization of core protein on RNA replication and protein synthesis. To clarify the reasons for the impaired growth of the M4243 virus in Vero cells, we measured viral RNA replication and protein synthesis in Vero and C6/36 cells infected with wild-type and M4243 viruses. It has been reported that the ratio of the positive strands to the negative strands of viral RNA in JEV-infected cells was 3:1 to 11.7:1 (58). Real-time RT-PCR specific for the negative-strand viral RNA used in this study is capable of detecting more than 10^2 copies/2 μl of the negative-sense viral RNA in the absence of the positive-strand RNA (Fig. 6A). The amounts of negative-strand RNA in the presence of a 100- or 1,000-fold excess amount of the positive-strand RNA were less than 10-fold different compared with those determined in the absence of the positive-strand RNA (Fig. 6A), indicating that the PCR system is specific enough to measure the negative-strand viral

RNA levels in cells infected with JEV. We then measured the synthesis of the negative-strand viral RNAs in Vero and C6/36 cells infected with wild-type or mutant JEV at an MOI of 5 by RT-PCR. Although similar levels of negative-strand RNA synthesis were observed in C6/36 cells infected with either virus, M4243 exhibited 3- and 18-fold-lower RNA replication than the wild type in Vero cells at 18 and 30 h postinoculation, respectively (Fig. 6B). Metabolic labeling of the host proteins indicated that there were no significant differences between the viabilities of Vero cells infected with wild-type and M4243 virus (data not shown). To determine the level of impairment of RNA translation of M4243 in Vero cells, viral protein syn-
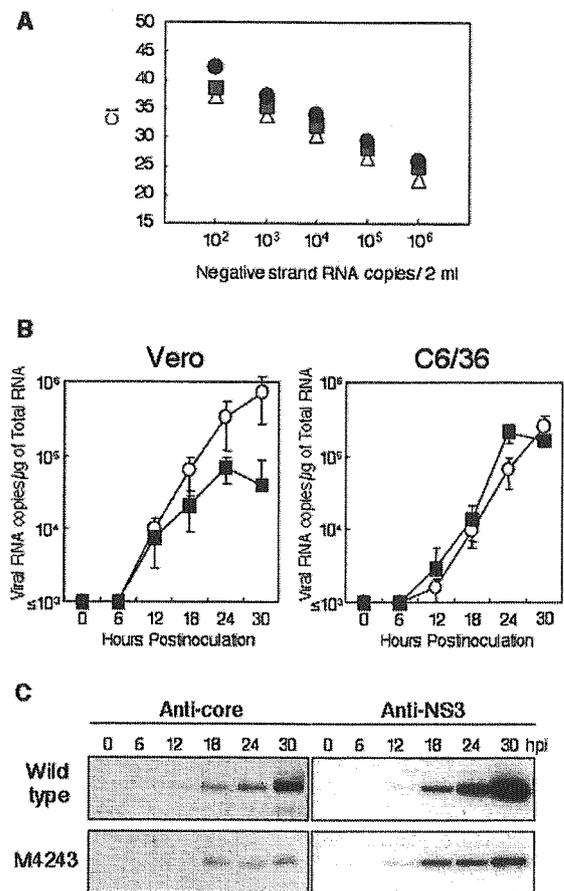

FIG. 6. Viral RNA and protein syntheses in Vero and C6/36 cells infected with wild-type or M4243 virus. (A) Establishment of negative-strand JEV RNA-specific real-time RT-PCR. A series of 10-fold dilutions of synthetic negative-strand RNA in the absence (closed circles) or presence of 100-fold (gray squares) or 1,000-fold (open triangles) synthetic positive-strand RNAs were applied to the real-time RT-PCR. The Ct value represents the first PCR cycle to detect the increase in signal associated with an exponential growth of PCR product. (B) Viral negative-strand RNAs were quantified in the infected cells by the real-time RT-PCR. Open circles and closed squares indicate wild-type and M4243 viruses, respectively. The detection limit was 10^3 copies of viral RNA/μg of total RNA. Means of three experiments are indicated. (C) Core and NS3 proteins were detected by Western blotting with anti-JEV core rabbit serum and anti-JEV NS3 MAb 34A1, respectively. A total of 4 μg of each sample was loaded.

theses in Vero cells infected with the wild-type or M4243 virus were analyzed by Western blotting (Fig. 6C). Although comparable amounts of core and NS3 proteins were detected at an early phase of infection (12 and 18 h postinoculation) in Vero cells infected with either virus, saturation of protein syntheses by a mutant virus was observed at 24 h postinfection, in contrast to cells infected with the wild-type virus, in which protein synthesis increased until 30 h postinfection. The early saturation of viral protein synthesis of M4243 in Vero cells is quite consistent with that of RNA replication. These results suggest that nuclear localization of the core protein plays a crucial role in the maintenance of replication-translation of viral RNA in mammalian cells but not in mosquito cells, in which the mutant virus replicates at a rate similar to that of the wild-type JEV.

Complementation of mutant virus replication by expression of the wild-type core protein. We next examined the growth of a mutant virus in cells transiently expressing the wild-type or mutant core protein. The efficiency of gene transduction into Vero cells is very low, and we therefore selected 293T cells for their high efficiency of foreign-gene transduction and used them to transiently express the JEV core protein. HA-tagged wild-type and mutant core proteins (approximately 16 kDa) and the viral core protein derived from M4243 (approximately 14 kDa) were detected in 293T cells transfected with the expression plasmids and infected with M4243 virus (Fig. 7A). Expression of the wild-type core protein, but not that of the mutant core protein, drastically enhanced viral growth of the M4243 virus up to the level of wild-type virus growth (Fig. 7B). However, the expression of the core proteins did not affect the replication of the wild-type virus. Furthermore, the negative-strand RNA synthesis of the mutant virus was increased threefold by the expression of the wild-type core protein, but not by that of the mutant protein, compared with mock-transfection results (Fig. 7C). These results indicate that the expression of the wild-type JEV core protein is able to compensate for the propagation of the M4243 virus.

Neurovirulence and neuroinvasiveness of M4243. To examine the neurovirulence characteristics of the wild-type and mutant viruses, we determined the LD_{50} values by intracerebral inoculation of the viruses into 3-week-old ICR mice. The LD_{50} values for the wild-type and the mutant viruses were 2.1 and 0.5 FFU, respectively. No significant differences in symptoms, mean duration period of diseases (wild versus mutant, 1.1 versus 0.9 days), and mean day of death (7.5 versus 7.6 days postinoculation) were observed between mice inoculated with 100 FFU of the wild-type virus and those inoculated with an equivalent dose of M4243 virus. To examine the growth kinetics of the viruses in the brain, 100 FFU of each virus was intracerebrally injected, and the viruses recovered from the brain homogenates were titrated. The growth of the M4243 virus was approximately 100 times lower than that of the wild-type virus (Fig. 8A, left panel), and revertant viruses exhibiting medium-sized plaques (Fig. 4B) were not recovered from the brains inoculated with the M4243 virus. The neuroinvasiveness of encephalitis flaviviruses is thought to be a reflection of their ability to grow in the peripheral organs, to breach the blood-brain barrier, and to infect central nervous systems following peripheral inoculation. To examine the neuroinvasiveness of wild-type and M4243 viruses, ICR mice were intraperitoneally
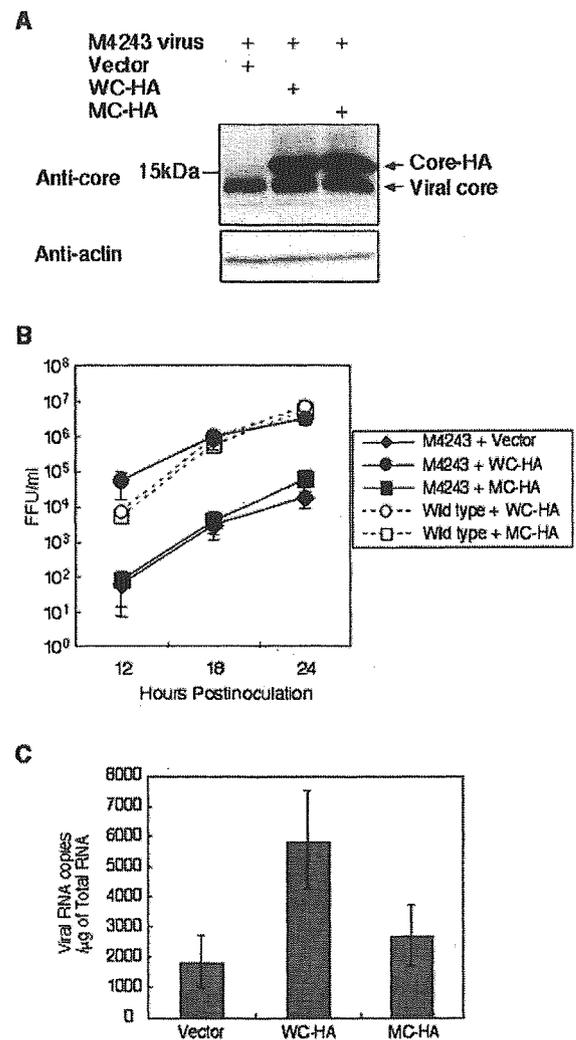

FIG. 7. Complementation of M4243 replication by expression of core proteins in 293T cells. At 4 h after transfection with pCAG-GS (Vector), pCAG-WC-HA (WC-HA), or pCAG-MC-HA (Gly^{42} and Pro^{43} to Ala) (MC-HA), 293T cells were infected with wild-type or M4243 virus at an MOI of 5. At 12, 18, or 24 h postinoculation, culture supernatants and cells were harvested to apply to focus-forming assays and Western blotting or real-time RT-PCR, respectively. (A) Western blotting of 293T cells transfected with plasmids expressing HA-tagged wild-type or mutant core protein and infected with M4243 virus. Molecular mass marker was indicated in the left of the panel. (B) Growth of wild-type and M4243 viruses in 293T cells transfected with the plasmids. Viral titers were determined by focus-forming assays in Vero cells. (C) Complementation of M4243 in 293T cells transfected with the plasmids at 24 h postinoculation. Viral RNA levels were determined by the negative-strand-specific real-time RT-PCR. Means from three experiments are indicated.

inoculated with 10^5 FFU of each virus. Only 1 of 11 mice inoculated with the M4243 virus had died by 9 days postinoculation, while on average 10 of the 11 mice inoculated with the wild-type virus had died by 9.6 days postinoculation (Fig. 8B). Over 5 days after inoculation, the viruses were recovered from the brain of mice inoculated with wild-type JEV but not from those inoculated with M4243 (Fig. 8A, right panel). These re-
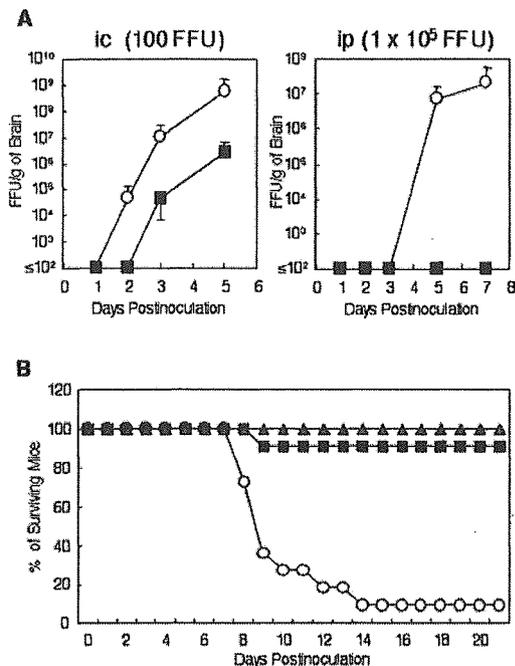
A

B

FIG. 8. Virulence of wild-type and M4243 viruses for ICR mice. (A) The infectious titers of wild-type and M4243 viruses in the brains of mice after inoculation with 100 FFU of the viruses intracerebrally (ic) or 10^5 FFU intraperitoneally (ip). Open circles and closed squares indicate wild-type and M4243 viruses, respectively. The detection limit is 10^2 FFU/gram of brain. Means of titers from four mice are indicated. (B) Percentages of surviving mice (10 to 11 mice per group) inoculated with 10^5 FFU of wild-type or M4243 viruses by an intraperitoneal route. Open circles, closed squares, and gray triangles indicate mice infected with the wild-type virus, infected with the M4243 virus, or mock infected, respectively.

sults indicated that the mutant virus exhibited a level of neurovirulence equivalent to that of the wild type but that its neuroinvasiveness was severely impaired in 3-week-old-ICR mice.

DISCUSSION

Like most animal RNA viruses, except for those of the families *Orthomyxoviridae*, *Bornaviridae*, and *Retroviridae*, members of the *Flaviviridae* replicate in the cytoplasm of host cells (34). However, it has been reported that the core proteins of DEN, KUN, and HCV are observed not only in the cytoplasm but also in the nucleus (4, 38, 55, 59, 61). In this study, we demonstrated that the JEV core protein was translocated into the nucleus and accumulated in the nucleolus of cells infected with JEV or transfected with an expression plasmid for the core protein. We revealed that Gly[42] and Pro[43] were important for the nuclear localization and that Gly[42] was essential for the nucleolar accumulation of the JEV core protein. The two amino acids Gly and Pro are well conserved not only among mosquitoborne flaviviruses such as JEV, KUN, WNV, and DEN but also among HCVs. According to the three-dimensional structures of KUN and DEN, the two amino acids are mapped to the unsheltered loop domain between α-helices 1 and 2 (11, 36). Substitutions of Gly[42] and Pro[43] with Ala completely abolished the nuclear localization of the JEV core pro-

tein as well as that of the DEN core protein (data not shown). However, a previous study showed that deletion of the N-terminal 45 amino acids of the DEN core protein did not eliminate nuclear localization of the protein (59). Although the reason for this discrepancy is not presently clear, our data suggest that the well-conserved Gly and Pro are important for nuclear or nucleolar localization of the core protein of flaviviruses. The two amino acids and the flanking sequences exhibited no similarity to the well-known classical NLSs, such as a large T-antigen of simian virus 40 (PKKKRKV) (21), nucleoplasmin (KRPAATKKAGQAKKKK) (5), and nucleolar localization signals, such as the Rex protein of human T-cell leukemia virus type I (MPKTRRRPRRSQRKRPPTP) (44). This domain may be required for recognition of novel nuclear import receptor protein(s) and nucleolar component(s). Recently, Dokland et al. demonstrated that tetramers of the KUN core protein extended as filamentous ribbon structures (11). The change of Gly[42] to Ala in the JEV core protein, therefore, may abolish the binding activity to nucleolar compartment(s) and exhibit a filamentous structure in the nuclei (Fig. 2C).

. The recovery of the M4243 virus in which Ala was substituted for Gly[42] and Pro[43] of the core protein suggests that nuclear localization of the core protein is not a necessary condition for viral propagation. However, replication of the mutant virus was impaired in mammalian cells but not in mosquito cells. The impairment of propagation of the M4243 virus in mammalian cells may be due to either of two phenomena: the decrease in production of infectious particles with a simultaneous increase of defective particles or the low efficiency of viral RNA replication. Since budding of flavivirus takes place through the interaction of prM and E proteins independently of the association with the core protein, disfunctions of core protein may reduce the production of infectious particles and enhance the production of subviral particles. In fact, mutations at the cleavage site of host signal peptidase in the core-prM junction of Murray Valley encephalitis virus caused an increase of subviral particle production (35). Furthermore, TBEV core proteins with deletions of the central hydrophobic region, containing Gly[36] corresponding to the Gly[42] essential for nucleolar localization of the JEV core protein, increased the production of subviral particles due to the lack of association with the ER membrane, where budding of the flavivirus takes place (26, 27). In contrast, the mutations on the Gly[42] and Pro[43] region of the JEV core protein caused the production of the defective particles different from subviral particles. Although the mechanisms underlying the production of the defective particles remain unclear, the mutations might affect the functions except for assembly and budding, such as maturation or uncoating. As far as we know, biological functions except for nuclear localization in the Gly[42] and Pro[43] region of the flavivirus core proteins have not been studied. The mutations might collaterally disrupt the conformation of the core protein essential for their functions of JEV. Meanwhile, it might be feasible that the nuclear localization of the core protein directly participates in the viral infectivity. Tijms et al. (56) demonstrated that the capsid protein of equine arteritis virus mostly shuffled between the cytoplasm and nucleus prior to cytoplasmic viral assembly, suggesting that the nuclear localization is crucial for viral assembly. In any case, production of the defective particles by the mutant JEV was enhanced in both Vero and C6/36 cells, and

thus, a decrease of infectious particles cannot explain the impairment of M4243 in Vero cells.

It is believed that the core protein is not required for RNA replication, since the RNA replicon of flavivirus, which does not contain the whole core gene, has been shown to be capable of replicating (10, 13, 24). Therefore, it is noteworthy that RNA replication of M4243 was impaired in Vero cells but not in mosquito cells. Although a cis-acting nucleotide sequence element essential for RNA replication has been mapped to the flavivirus core genes (10, 22), the nucleotide changes were not involved in the impairment of replication of M4243 due to the compensation of RNA replication by the expression of wild-type core protein in trans. The kinetics study of viral RNA and protein syntheses suggested that the JEV core protein translated at the early step of infection was translocated into the nucleus and enhanced RNA replication at the late phase of infection, although further studies are needed to clarify the precise mechanism. Earlier studies (30, 31) resulted in reports that flaviviruses, including JEV, but not alphaviruses failed to propagate and produce viral antigens in cells enucleated by cytochalasin B, suggesting the involvement of host nucleus factors in flavivirus replication. The DEN core protein was reported to interact with a nuclear transcription factor, heterogeneous nuclear ribonucleoprotein K, and regulate the C/EBP-β-mediated transcription (7). Furthermore, the HCV core protein was also shown to associate with host nuclear proteins such as heterogeneous nuclear ribonucleoprotein K (18) and PA28γ (42) and was suggested to regulate the transcription of host cells (18, 45). The nuclear localization of core proteins of Flaviviridae might change the suitability of the host-cell environment for viral propagation by producing factors that enhance RNA replication or by suppressing those that reduce it.

Other cytoplasmic RNA viruses, such as members of the families Picornaviridae (1, 2, 12), Coronaviridae (8, 15, 62), Arteriviridae (48, 56), Togaviridae (41), and Rhabdoviridae (46), may also feed their proteins into the nucleus to facilitate viral propagation. For example, it is suggested that the protein 2A of encephalomyocarditis virus is localized to the nucleoli and inhibits cellular mRNA transcription (1) and that point mutations within the NLS of another nucleolar protein, 3D^{pol}, were lethal due to the inhibition of viral RNA replication (2). The coronavirus nucleoproteins were also found to be localized in the nucleoli of the host cells (8, 15, 62), and the expression of the coronavirus nucleoproteins by transfection inhibits host cell division (8, 62).

Surprisingly, the M4243 virus exhibited a high level of neurovirulence in mice comparable to that of the wild-type JEV despite the fact that the M4243 virus had a 100-fold-lower replication efficiency than the wild-type JEV in vivo. Encephalitis induced by flavivirus infection is thought to arise from direct injury of brain neurons by viral replication (49, 64) or indirect injury of brain neurons by immune responses (60). However, the idea that the direct injury of neurons is responsible for encephalitis induced by flavivirus is difficult to reconcile with the results showing that the virulence of the M4243 virus is equivalent to that of the wild-type virus. A previous study indicated that a low dose of WNV-induced encephalitis was associated with inflammatory cell infiltration in mice (60). Alternatively, the defective particles contained in the inoculum or produced by M4243 infections might stimulate a signal pathway via reactive oxygen species in neuronal cells and induce cell death, as described by Lin et al. (33).

In contrast to the neurovirulence results, a striking difference in levels of neuroinvasiveness was observed between the wild-type and M4243 viruses. Although the magnitude and duration of viremia were suggested to be major determinants for neuroinvasion (19, 32), the precise mechanism by which flaviviruses breach the blood-brain barrier and enter the brain tissue remains uncertain. Encephalitis flaviviruses injected by peripheral routes are thought to replicate in lymphatic tissues, such as peripheral lymph nodes or spleen, and to induce further viremia (32, 40). Although we had no evidence that JEV replicated in peripheral tissues prior to neuroinvasion as described by others (32), the wild-type virus, but not M4243, was present in small amounts (100 to 200 FFU/ml) in blood samples at 1 and 3 days postinoculation (data not shown). In this context, it might be possible that the M4243 virus was unable to replicate in peripheral tissues at a level sufficient to develop viremia and breach the blood-brain barrier, resulting in the low level of neuroinvasiveness. The novel attenuation of neuroinvasiveness observed in M4243 may be applicable to the development of new live vaccines against flavivirus infection.

The life cycles of most flaviviruses are sustained between arthropods and vertebrates. The present finding that nuclear localization of the core protein enhances viral replication in mammalian cells may lead to an improved understanding of the evolutionary adaptation strategy of flaviviruses in expanding their host range from arthropods to vertebrates. It might also be possible to speculate that JEV transgressed its host barrier by translocating the core protein into the nucleus of porcine cells and incorporated the pig as an amplifier in the life cycle of JEV. Furthermore, it is of interest for evolutional studies on the family Flaviviridae that the NLSs of core proteins were well conserved between mosquitoborne flaviviruses and bloodborne and human-adapted HCV.

REFERENCES

1. Aminev, A. G., S. P. Amineva, and A. C. Palmenberg. 2003. Encephalomyocarditis viral protein 2A localizes to nucleoli and inhibits cap-dependent mRNA translation. Virus Res. 95:45–57.
2. Aminev, A. G., S. P. Amineva, and A. C. Palmenberg. 2003. Encephalomyocarditis virus (EMCV) proteins 2A and 3BCD localize to nuclei and inhibit cellular mRNA transcription but not rRNA transcription. Virus Res. 95:59–73.
3. Brooks, P., G. Fuertes, R. Z. Murray, S. Bose, E. Knecht, M. C. Rechsteiner, K. B. Hendil, K. Tanaka, J. Dyson, and J. Rivett. 2000. Subcellular localization of proteasomes and their regulatory complexes in mammalian cells. Biochem. J. 346:155–161.
4. Bulich, R., and J. G. Aaskov. 1992. Nuclear localization of dengue 2 virus core protein detected with monoclonal antibodies. J. Gen. Virol. 73:2999–3003.
5. Bürglin, T. R., and E. M. De Robertis. 1987. The nuclear migration signal of Xenopus laevis nucleoplasmin. EMBO J. 6:2617–2625.
6. Burke, D. S., and T. P. Monath. 2001. Flaviviruses, p. 1043–1125. In D. M. Knipe, P. M. Howley, D. E. Griffin, R. A. Lamb, M. A. Martin, B. Roizman,

and S. E. Straus (ed.), Fields virology, 4th ed., vol. 1. Lippincott Williams & Wilkins, Philadelphia, Pa.

7. Chang, C. J., H. W. Luh, S. H. Wang, H. J. Lin, S. C. Lee, and S. T. Hu. 2001. The heterogeneous nuclear ribonucleoprotein K (hnRNP K) interacts with dengue virus core protein. DNA Cell Biol. 20:569–577.

8. Chen, H., T. Wurm, P. Britton, G. Brooks, and J. A. Hiscox. 2002. Interaction of the coronavirus nucleoprotein with nucleolar antigens and the host cell. J. Virol. 76:5233–5250.

9. Clarke, D. H., and J. Casals. 1958. Techniques for hemagglutination and hemagglutination-inhibition with arthropod-borne viruses. Am. J. Trop. Med. Hyg. 7:561–573.

10. Corver, J., E. Lenches, K. Smith, R. A. Robison, T. Sando, E. G. Strauss, and J. H. Strauss. 2003. Fine mapping of a cis-acting sequence element in yellow fever virus RNA that is required for RNA replication and cyclization. J. Virol. 77:2265–2270.

11. Dokland, T., M. Walsh, J. M. Mackenzie, A. A. Khromykh, K. H. Ee, and S. Wang. 2004. West Nile virus core protein: tetramer structure and ribbon formation. Structure 12:1157–1163.

12. Fernandez-Tomas, C. 1982. The presence of viral-induced proteins in nuclei from poliovirus-infected HeLa cells. Virology 116:629–634.

13. Gehrke, R., M. Ecker, S. W. Aberle, S. L. Allison, F. X. Heinz, and C. W. Mandl. 2003. Incorporation of tick-borne encephalitis virus replicons into virus-like particles by a packaging cell line. J. Virol. 77:8924–8933.

14. Higuchi, R., B. Krummel, and R. K. Saiki. 1988. A general method of in vitro preparation and specific mutagenesis of DNA fragments: study of protein and DNA interactions. Nucleic Acids Res. 16:7351–7367.

15. Hiscox, J. A., T. Wurm, L. Wilson, P. Britton, D. Cavanagh, and G. Brooks. 2001. The coronavirus infectious bronchitis virus nucleoprotein localizes to the nucleolus. J. Virol. 75:506–512.

16. Ho, S. N., H. D. Hunt, R. M. Horton, J. K. Pullen, and L. R. Pease. 1989. Site-directed mutagenesis by overlap extension using the polymerase chain reaction. Gene 77:51–59.

17. Horton, R. M., H. D. Hunt, S. N. Ho, J. K. Pullen, and L. R. Pease. 1989. Engineering hybrid genes without the use of restriction enzymes: gene splicing by overlap extension. Gene 77:61–68.

18. Hsieh, T. Y., M. Matsumoto, H. C. Chou, R. Schneider, S. B. Hwang, A. S. Lee, and M. M. Lai. 1998. Hepatitis C virus core protein interacts with heterogeneous nuclear ribonucleoprotein K. J. Biol. Chem. 273:17651–17659.

19. Huang, C. H., and C. Wong. 1963. Relation of the peripheral multiplication of Japanese B encephalitis virus to the pathogenesis of the infection in mice. Acta Virol. 7:322–330.

20. Jones, C. T., L. Ma, J. W. Burgner, T. D. Groesch, C. B. Post, and R. J. Kuhn. 2003. Flavivirus capsid is a dimeric alpha-helical protein. J. Virol. 77:7143–7149.

21. Kalderon, D., W. D. Richardson, A. F. Markham, and A. E. Smith. 1984. Sequence requirements for nuclear location of simian virus 40 large-T antigen. Nature 311:33–38.

22. Khromykh, A. A., H. Meka, K. J. Guyatt, and E. G. Westaway. 2001. Essential role of cyclization sequences in flavivirus RNA replication. J. Virol. 75:6719–6728.

23. Khromykh, A. A., and E. G. Westaway. 1996. RNA binding properties of core protein of the flavivirus Kunjin. Arch. Virol. 141:685–699.

24. Khromykh, A. A., and E. G. Westaway. 1997. Subgenomic replicons of the flavivirus Kunjin: construction and applications. J. Virol. 71:1497–1505.

25. Kofler, R. M., J. H. Aberle, S. W. Aberle, S. L. Allison, F. X. Heinz, and C. W. Mandl. 2004. Mimicking live flavivirus immunization with a noninfectious RNA vaccine. Proc. Natl. Acad. Sci. USA 101:1951–1956.

26. Kofler, R. M., F. X. Heinz, and C. W. Mandl. 2002. Capsid protein C of tick-borne encephalitis virus tolerates large internal deletions and is a favorable target for attenuation of virulence. J. Virol. 76:3534–3543.

27. Kofler, R. M., A. Leitner, G. O'Riordain, F. X. Heinz, and C. W. Mandl. 2003. Spontaneous mutations restore the viability of tick-borne encephalitis virus mutants with large deletions in protein C. J. Virol. 77:443–451.

28. Konishi, E., S. Pincus, B. A. Fonseca, R. E. Shope, E. Paoletti, and P. W. Mason. 1991. Comparison of protective immunity elicited by recombinant vaccinia viruses that synthesize E or NS1 of Japanese encephalitis virus. Virology 185:401–410.

29. Konishi, E., S. Pincus, E. Paoletti, R. E. Shope, T. Burrage, and P. W. Mason. 1992. Mice immunized with a subviral particle containing the Japanese encephalitis virus prM/M and E proteins are protected from lethal JEV infection. Virology 188:714–720.

30. Kos, K. A., B. A. Osborne, and R. A. Goldsby. 1975. Inhibition of group B arbovirus antigen production and replication in cells enucleated with cytochalasin B. J. Virol. 15:913–917.

31. Lad, V. J., A. K. Gupta, S. N. Ghosh, and K. Banerjee. 1993. Immunofluorescence studies on the replication of some arboviruses in nucleated and enucleated cells. Acta Virol. 37:79–83.

32. Lee, E., and M. Lobigs. 2002. Mechanism of virulence attenuation of glycosaminoglycan-binding variants of Japanese encephalitis virus and Murray Valley encephalitis virus. J. Virol. 76:4901–4911.

33. Lin, R. J., C. L. Liao, and Y. L. Lin. 2004. Replication-incompetent virions

of Japanese encephalitis virus trigger neuronal cell death by oxidative stress in a culture system. J. Gen. Virol. 85:521–533.

34. Lindenbach, B. D., and C. M. Rice. 2001. Flaviviridae: The viruses and their replication, p. 991–1041. In D. M. Knipe, P. M. Howley, D. E. Griffin, R. A. Lamb, M. A. Martin, B. Roizman, and S. E. Straus (ed.). Fields virology, 4th ed., vol. 1. Lippincott Williams & Wilkins, Philadelphia, Pa.

35. Lobigs, M., and E. Lee. 2004. Inefficient signalase cleavage promotes efficient nucleocapsid incorporation into budding flavivirus membranes. J. Virol. 78:178–186.

36. Ma, L., C. T. Jones, T. D. Groesch, R. J. Kuhn, and C. B. Post. 2004. Solution structure of dengue virus capsid protein reveals another fold. Proc. Natl. Acad. Sci. USA 101:3414–3419.

37. Macara, I. G. 2001. Transport into and out of the nucleus. Microbiol. Mol. Biol. Rev. 65:570–594.

38. Makino, Y., M. Tadano, T. Anzai, S. P. Ma, S. Yasuda, and T. Fukunaga. 1989. Detection of dengue 4 virus core protein in the nucleus. II. Antibody against dengue 4 core protein produced by a recombinant baculovirus reacts with the antigen in the nucleus. J. Gen. Virol. 70:1417–1425.

39. Markoff, L., B. Falgout, and A. Chang. 1997. A conserved internal hydrophobic domain mediates the stable membrane integration of the dengue virus capsid protein. Virology 233:105–117.

40. McMinn, P. C., L. Dalgarno, and R. C. Weir. 1996. A comparison of the spread of Murray Valley encephalitis viruses of high or low neuroinvasiveness in the tissues of Swiss mice after peripheral inoculation. Virology 220:414–423.

41. Michel, M. R., M. Elgizoli, Y. Dai, R. Jakob, H. Koblet, and A.-P. Arrigo. 1990. Karyophilic properties of Semliki Forest virus nucleocapsid protein. J. Virol. 64:5123–5131.

42. Moriishi, K., T. Okabayashi, K. Nakai, K. Moriya, K. Koike, S. Murata, T. Chiba, K. Tanaka, R. Suzuki, T. Suzuki, T. Miyamura, and Y. Matsuura. 2003. Proteasome activator PA28γ-dependent nuclear retention and degradation of hepatitis C virus core protein. J. Virol. 77:10237–10249.

43. Niwa, H., K. Yamamura, and J. Miyazaki. 1991. Efficient selection for high-expression transfectants with a novel eukaryotic vector. Gene 108:193–199.

44. Nosaka, T., H. Siomi, Y. Adachi, M. Ishibashi, S. Kubota, M. Maki, and M. Hatanaka. 1989. Nucleolar targeting signal of human T-cell leukemia virus type I rex-encoded protein is essential for cytoplasmic accumulation of unspliced viral mRNA. Proc. Natl. Acad. Sci. USA 86:9798–9802.

45. Otsuka, M., N. Kato, K. Lan, H. Yoshida, J. Kato, T. Goto, Y. Shiratori, and M. Omata. 2000. Hepatitis C virus core protein enhances p53 function through augmentation of DNA binding affinity and transcriptional ability. J. Biol. Chem. 275:34122–34130.

46. Petersen, J. M., L. S. Her, V. Varvel, E. Lund, and J. E. Dahlberg. 2000. The matrix protein of vesicular stomatitis virus inhibits nucleocytoplasmic transport when it is in the nucleus and associated with nuclear pore complexes. Mol. Cell. Biol. 20:8590–8601.

47. Reed, L. J., and H. Muench. 1938. A simple method of estimating fifty per cent endpoints. Am. J. Hyg. 27:493.

48. Rowland, R. R., R. Kervin, C. Kuckleburg, A. Sperlich, and D. A. Benfield. 1999. The localization of porcine reproductive and respiratory syndrome virus nucleocapsid protein to the nucleolus of infected cells and identification of a potential nucleolar localization signal sequence. Virus Res. 64:1–12.

49. Shrestha, B., D. Gottlieb, and M. S. Diamond. 2003. Infection and injury of neurons by West Nile encephalitis virus. J. Virol. 77:13203–13213.

50. Solomon, T., H. Ni, D. W. Beasley, M. Ekkelenkamp, M. J. Cardosa, and A. D. Barrett. 2003. Origin and evolution of Japanese encephalitis virus in southeast Asia. J. Virol. 77:3091–3098.

51. Spector, D. L., R. L. Ochs, and H. Busch. 1984. Silver staining, immunofluorescence, and immunoelectron microscopic localization of nucleolar phosphoproteins B23 and C23. Chromosoma 90:139–148.

52. Stocks, C. E., and M. Lobigs. 1998. Signal peptidase cleavage at the flavivirus C-prM junction: dependence on the viral NS2B-3 protease for efficient processing requires determinants in C, the signal peptide, and prM. J. Virol. 72:2141–2149.

53. Sumiyoshi, H., C. Mori, I. Fuke, K. Morita, S. Kuhara, J. Kondou, Y. Kikuchi, H. Nagamatu, and A. Igarashi. 1987. Complete nucleotide sequence of the Japanese encephalitis virus genome RNA. Virology 161:497–510.

54. Suzuki, R., Y. Matsuura, T. Suzuki, A. Ando, J. Chiba, S. Harada, I. Saito, and T. Miyamura. 1995. Nuclear localization of the truncated hepatitis C virus core protein with its hydrophobic C terminus deleted. J. Gen. Virol. 76:53–61.

55. Tadano, M., Y. Makino, T. Fukunaga, Y. Okuno, and K. Fukai. 1989. Detection of dengue 4 virus core protein in the nucleus. I. A monoclonal antibody to dengue 4 virus reacts with the antigen in the nucleus and cytoplasm. J. Gen. Virol. 70:1409–1415.

56. Tijms, M. A., Y. van der Meer, and E. J. Snijder. 2002. Nuclear localization of non-structural protein 1 and nucleocapsid protein of equine arteritis virus. J. Gen. Virol. 83:795–800.

57. Tsai, T. F. 2000. New initiatives for the control of Japanese encephalitis by vaccination: minutes of a W.H.O./CVI meeting, Bangkok, Thailand, 13–15 October 1998. Vaccine 18:1–25.

58. Uchil, P. D., and V. Satchidanandam. 2003. Architecture of the flaviviral replication complex. Protease, nuclease, and detergents reveal encasement

within double-layered membrane compartments. J. Biol. Chem. **278:**24388–24398.

59. **Wang, S. H., W. J. Syu, K. J. Huang, H. Y. Lei, C. W. Yao, C. C. King, and S. T. Hu.** 2002. Intracellular localization and determination of a nuclear localization signal of the core protein of dengue virus. J. Gen. Virol. **83:**3093–3102.

60. **Wang, Y., M. Lobigs, E. Lee, and A. Mullbacher.** 2003. CD8$^+$ T cells mediate recovery and immunopathology in West Nile virus encephalitis. J. Virol. **77:**13323–13334.

61. **Westaway, E. G., A. A. Khromykh, M. T. Kenney, J. M. Mackenzie, and M. K. Jones.** 1997. Proteins C and NS4B of the flavivirus Kunjin translocate independently into the nucleus. Virology **234:**31–41.

62. **Wurm, T., H. Chen, T. Hodgson, P. Britton, G. Brooks, and J. A. Hiscox.** 2001. Localization to the nucleolus is a common feature of coronavirus nucleoproteins, and the protein may disrupt host cell division. J. Virol. **75:**9345–9356.

63. **Yamshchikov, V. F., and R. W. Compans.** 1994. Processing of the intracellular form of the West Nile virus capsid protein by the viral NS2B-NS3 protease: an in vitro study. J. Virol. **68:**5765–5771.

64. **Yang, K. D., W. T. Yeh, R. F. Chen, H. L. Chuon, H. P. Tsai, C. W. Yao, and M. F. Shaio.** 2004. A model to study neurotropism and persistency of Japanese encephalitis virus infection in human neuroblastoma cells and leukocytes. J. Gen. Virol. **85:**635–642.

Molecular Determinants for Subcellular Localization of Hepatitis C Virus Core Protein

Ryosuke Suzuki,[1] Shinichiro Sakamoto,[1] Takeya Tsutsumi,[1] Akiko Rikimaru,[1,2] Keiko Tanaka,[3]
Takashi Shimoike,[1] Kohji Moriishi,[4] Takuya Iwasaki,[3,5] Kiyohisa Mizumoto,[2]
Yoshiharu Matsuura,[4] Tatsuo Miyamura,[1] and Tetsuro Suzuki[1]*

*Department of Virology II, National Institute of Infectious Diseases, Shinjuku-ku,[1] Department of Biochemistry, School of
Pharmaceutical Sciences, Kitasato University, Minato-ku,[2] and Department of Pathology, National Institute of Infectious
Diseases, Shinjuku-ku,[3] Tokyo, Research Center for Emerging Infectious Diseases, Research Institute for
Microbial Diseases, Osaka University, Suita-shi, Osaka,[4] and Department of Pathology, Institute of
Tropical Medicine, Nagasaki University, Nagasaki-shi, Nagasaki,[5] Japan*

Hepatitis C virus (HCV) core protein is a putative nucleocapsid protein with a number of regulatory functions. In tissue culture cells, HCV core protein is mainly located at the endoplasmic reticulum as well as mitochondria and lipid droplets within the cytoplasm. However, it is also detected in the nucleus in some cells. To elucidate the mechanisms by which cellular trafficking of the protein is controlled, we performed subcellular fractionation experiments and used confocal microscopy to examine the distribution of heterologously expressed fusion proteins involving various deletions and point mutations of the HCV core combined with green fluorescent proteins. We demonstrated that a region spanning amino acids 112 to 152 can mediate association of the core protein not only with the ER but also with the mitochondrial outer membrane. This region contains an 18-amino-acid motif which is predicted to form an amphipathic α-helix structure. With regard to the nuclear targeting of the core protein, we identified a novel bipartite nuclear localization signal, which requires two out of three basic-residue clusters for efficient nuclear translocation, possibly by occupying binding sites on importin-α. Differences in the cellular trafficking of HCV core protein, achieved and maintained by multiple targeting functions as mentioned above, may in part regulate the diverse range of biological roles of the core protein.

Hepatitis C virus (HCV), the most important causative agent of posttransfusion and sporadic non-A, non-B hepatitis, is a positive-stranded RNA virus belonging to the family *Flaviviridae* (7). A precursor polyprotein of about 3,000 amino acids is encoded by a large open reading frame of the genome and undergoes cellular and viral protease-mediated posttranslational modification to produce a series of structural and nonstructural proteins (8, 13, 16).

HCV core protein, which is derived from the N terminus of the viral polyprotein, forms multimers and interacts physically with the viral RNA to constitute the nucleocapsid (28, 47, 50). Tissue transglutaminase is responsible for stabilizing the core protein by cross-linking it into a dimeric form (26). In addition, the core viral protein has properties which enable it to modulate a number of cellular processes, including transcription, inhibition or stimulation of apoptosis, and suppression of host immunity, as reviewed previously (21, 29, 51, 52). Several studies suggest that expression of the core protein affects mitochondrial function and lipid metabolism. The core protein increases the cellular production of reactive oxygen species with subsequent increases in lipid peroxidation (35, 39). The viral protein also colocalizes with human apolipoprotein AII, associates with lipid droplets, and has the capacity to influence

metabolic events involving lipid storage (2, 17, 30, 36, 44). In addition, the core protein reduces microsomal triglyceride transfer, leading to defects in very low density lipoprotein assembly and secretion (40). Furthermore, the HCV core protein has transforming potential in some cells under certain conditions (5, 42). Transgenic mice expressing this protein in the liver develop hepatic steatosis due to increased oxidative stress in the absence of inflammation, with subsequent development of hepatocellular carcinoma (34, 36). These results suggest that the HCV core protein might play a pivotal role in the pathogenesis of hepatitis C in addition to its role as a structural component of the viral capsid.

The amino acid sequence of the core protein is well conserved among different HCV isolates and genotypes compared to other HCV proteins. The N-terminal domain of the HCV core protein is highly basic, while its C terminus is hydrophobic. Although several core proteins of various sizes exist (17 to 23 kDa) (15, 23, 25, 49, 56), two processing events result in the predominant production of a 21-kDa core protein. Both of these events utilize the endoplasmic reticulum (ER). The first one is to be cleaved from downstream envelope protein E1 at position 191, where the C-terminal hydrophobic domain serves as a putative signal peptide sequence. Subsequently, the signal sequence of 13 or 18 residues is processed by signal peptide peptidase (19, 23, 56).

The HCV core protein is found primarily within the membranes of cytoplasmic organelles, but it is also found in the nucleus (23, 48, 56). Immunofluorescence studies show a punc-

* Corresponding author. Mailing address: Department of Virology II, National Institute of Infectious Diseases, 1-23-1 Toyama, Shinjuku-ku, Tokyo, Japan 162-8640. Phone: (81) 3-5285-1111. Fax: (81) 3-5285-1161. E-mail: tesuzuki@nih.go.jp.

tate pattern, consistent with ER localization, as well as perinuclear localization (15, 24, 32, 46, 56). Some studies suggest direct effects of the core protein on mitochondrial function. In fact, the core protein localizes to the mitochondria (34, 39). The N-terminal domain of the core protein contains three stretches of arginine- and lysine-rich sequences. Translocation of the core protein to the nucleus, mediated by these basic-residue stretches which function as nuclear localization signals (NLSs), is observed (6, 48). In addition, Moriishi et al. demonstrated that the N-terminal region of the core protein is also essential for nuclear retention through its interaction with the proteasome activator PA28γ (33).

In this study, we found a region that is important for localization of the mature core protein to the ER and to the mitochondrial outer membrane. We also identified a novel bipartite NLS responsible for nuclear targeting of the core protein, presumably via an importin-dependent pathway.

MATERIALS AND METHODS

Plasmid construction. The construction of a plasmid expressing the full-length core protein of 191 amino acids, pCAGC191, was described previously (49). pGFP, a construct expressing green fluorescent protein (GFP) with a C-terminal Myc epitope tag sequences, was prepared as follows. pCMV/Myc/mito/GFP (Invitrogen Corp., Carlsbad, Calif.) was digested with PmlI, followed by treatment with the Klenow fragment of DNA polymerase I. The resultant linear fragment was ligated to a PstI linker (GCTGCAGC) and digested with PstI to remove the mitochondrial targeting signal sequence, followed by self-ligation. A series of HCV core-GFP fusion constructs were made by amplifying the core gene fragments with PCR with primers containing Flag epitope tag sequences (sense) and a PstI site (both). After digestion with PstI, the segments were inserted into the PstI site of pGFP. A series of GFP-core-E1 fusion constructs were made by amplifying core and E1 gene fragments with PCR with primers containing a NotI site. After digestion with NotI, the segments were inserted into the NotI site of pGFP.

pGEX-4T-1 (Amersham Bioscience Corp., Piscataway, N.J.) was used to express core protein fused with glutathione S-transferase (GST) in *Escherichia coli*. Core cDNA fragments encoding amino acids 1 to 71 were inserted into the EcoRI site of pGEX-4T-1. Alanine substitutions were introduced into the core protein by PCR mutagenesis with primers containing base alterations. The PCR products were then cloned into pCR2.1 (Invitrogen Corp.) and verified by DNA sequencing. Individual cDNAs were excised and inserted separately into pGFP or pGEX-4T-1. The primer sequences used in this study are available from the authors upon request.

Plasmid pRSET-hSRP1α (54), containing importin-α cDNA under the control of a T7 promoter, was kindly provided by Karsten Weis (University of California, Berkeley). A cDNA clone of importin-α possessing 14 residues (MYPYDVP DYGGGGS), derived in part from the hemagglutinin (HA) tag at the N terminus, was constructed by PCR. The resultant linear fragment was inserted under the control of a CAG promoter of pCAGGS and designated pCAG-HA-imp.

Cell culture and transfection. Human embryonic kidney 293T cells were maintained in Dulbecco's modified Eagle's medium supplemented with 100 units of penicillin per ml, 100 μg of streptomycin per ml, and 10% fetal bovine serum at 37°C in a 5% CO_2 incubator. Monolayers of 293T cells were transfected with plasmid DNA in the presence of Lipofectamine (Gibco-BRL, Life Technologies, Gaithersburg, Md.) according to the manufacturer's instructions.

Confocal immunofluorescence microscopy. Transfected cells were grown on glass coverslips. Two days after transfection, cells were fixed with 4% paraformaldehyde in phosphate-buffered saline (PBS) for 20 min at room temperature. Intracellular localization of HCV core-GFP fusion proteins was visualized in cells transfected with a variety of GFP fusion constructs.

In order to detect the HCV core protein by immunofluorescence, fixed cells were permeabilized with 0.2% Triton X-100 in PBS for 3 min at room temperature, followed by blocking with a nonfat milk solution (Block Ace; Snow Brand Milk Products Co., Sapporo, Japan). The cells were then incubated with anticore monoclonal antibody B2 (Anogen, Mississauga, Canada) for 60 min at room temperature, followed by incubation with fluorescein isothiocyanate-conjugated rabbit anti-mouse immunoglobulin G (IgG) (ICN Pharmaceuticals, Aurora, Ohio) for 45 min. To visualize mitochondria, MitoTracker Red CM-H_2XRos

(Molecular Probes, Eugene, Oreg.) was added to the culture medium to a final concentration of 100 nM and incubated for 120 min at 37°C prior to fixation. To visualize the ER, goat anticalregulin antibody (Santa Cruz Biotechnology, Santa Cruz, Calif.) and rhodamine-conjugated rabbit anti-goat IgG (ICN Pharmaceuticals) were used as the first and second antibodies, respectively. To visualize HA-importin-α, mouse anti-HA antibody (Roche Molecular Biochemicals, Indianapolis, Ind.) and rhodamine-conjugated goat anti-mouse IgG (ICN Pharmaceuticals) were used as the first and second antibodies, respectively. All specimens were examined with an LSM510 laser scanning confocal microscope (Carl Zeiss, Oberkochen, Germany).

Immunoelectron microscopy. Cells were transfected as described above. After 2 days, cells were fixed with 3% paraformaldehyde and 0.1% glutaraldehyde in 0.1 M PBS (pH 7.4). Free aldehyde groups were quenched with 50 mM NH_4Cl in PBS. The cell pellets were embedded at progressively lower temperatures (down to $-35°C$) in Lowicryl k4M according to an established protocol (43). Ultrathin sections were prepared and mounted on carbon-coated nickel grids. To perform electron microscopy, Lowicryl k4M ultrathin sections, mounted on grids, were floated on a droplet of PBS containing 1% bovine serum albumin, 0.1% Triton X-100, and 0.1% Tween 20 for 10 min, after which they were exposed to droplets of mouse anticore monoclonal antibody (Anogen) diluted in PBS for 45 min. Following this, they were rinsed twice for 5 min each in PBS and incubated with anti-mouse IgG-coated 10-nm immunogold particles (British Biocell, Cardiff, United Kingdom) for 45 min. After rinsing with PBS and distilled water, the grids and embedded sections were air dried and exposed to uranyl and lead acetate contrast agents.

Subcellular fractionation. All steps were performed at 4°C in the presence of a protease inhibitor cocktail called Complete (Roche Molecular Biochemicals). To isolate the ER fraction, transfected cells were washed with PBS, lysed in homogenization buffer A (50 mM Tris-HCl [pH 8.0], 1 mM β-mercaptoethanol, 1 mM EDTA, and 0.32 M sucrose), and then centrifuged at 5,000 × g for 10 min. The supernatant was then collected and centrifuged at 105,000 × g for 1 h. The pellet was disrupted in lysis buffer (50 mM Tris-HCl [pH 7.5], 150 mM NaCl, 1% NP-40, 1 mM dithiothreitol, 1 mM sodium orthovanadate, and 10 mM sodium fluoride), after which it was centrifuged at 15,000 × g for 20 min. The resulting supernatant was used as the ER fraction.

To isolate the mitochondrial fraction, transfected cells were washed with PBS and homogenized in ice-cold homogenization buffer B (200 mM mannitol, 50 mM sucrose, 1 mM EDTA, and 10 mM Tris-HCl) at pH 7.4. The supernatant was then centrifuged at 1,000 × g for 10 min to remove large debris and nuclei. The resulting supernatant was then centrifuged at 20,000 × g for 20 min to obtain crude mitochondria. The crude mitochondria pellet was subfractionated in Nycodenz gradients for further purification of mitochondria. Nycodenz (Axis-Shield PoC AS, Oslo, Norway) solution at 50% (wt/vol) was prepared in buffer containing 5 mM Tris-HCl and 1 mM EDTA at pH 7.4. This stock solution was then diluted with buffer containing 0.25 M sucrose, 5 mM Tris-HCl, and 1 mM EDTA at pH 7.4 before use. The crude mitochondrial pellets was suspended in 4 ml of 25% Nycodenz solution and overlaid onto the following discontinuous Nycodenz gradients: 1 ml of 40%, 1 ml of 34%, and 2 ml of 30%. The samples were topped off with 2 ml of 23% Nycodenz solution after placement onto the discontinuous gradients. The tubes were then centrifuged at 52,000 × g for 90 min. The dense band seen after centrifugation at the 25 to 30% interface was recovered as the purified mitochondrial fraction.

To determine the submitochondrial localization pattern of the core protein, mitochondria were resuspended in SH buffer (0.6 M sorbitol and 20 mM HEPES-KOH [pH 7.2]) in the absence or presence of 30 μg of proteinase K per ml after purification by Nycodenz density gradient centrifugation. Samples were incubated for 30 min at 0°C, after which protease digestion was halted by the addition of p-aminophenyl methanesulfonyl fluoride hydrochloride (p-APMSF) (5 mM). Proteins lysed in sodium dodecyl sulfate (SDS) sample buffer were analyzed by SDS-polyacrylamide gel electrophoresis (PAGE) and immunoblotted as described below.

Immunoblot analysis. The proteins were transferred to a polyvinylidene difluoride membrane (Immobilon; Millipore, Tokyo, Japan) after separation by SDS-PAGE. After blocking, the membranes were probed with monoclonal- or polyclonal-antibody against core protein (Anogen), prohibitin (Neo Markers, Fremont, Calif.), ribophorin I (Santa Cruz Biotechnology), translocase of the outer membrane (Tom) 20 (Santa Cruz Biotechnology), translocase of the inner membrane (Tim) 17 (Santa Cruz Biotechnology), or GFP (Santa Cruz Biotechnology). Immunoblots were developed as previously described (15).

GST pulldown assay. *Escherichia coli* BL21 cells were transformed with GST-core fusion plasmids and grown at 37°C. Expression of the fusion protein was induced by 1 mM isopropyl-β-D-thiogalactopyranoside at 37°C for 3 h. Bacteria were harvested, suspended in lysis buffer (1% Triton X-100 in PBS), and soni-
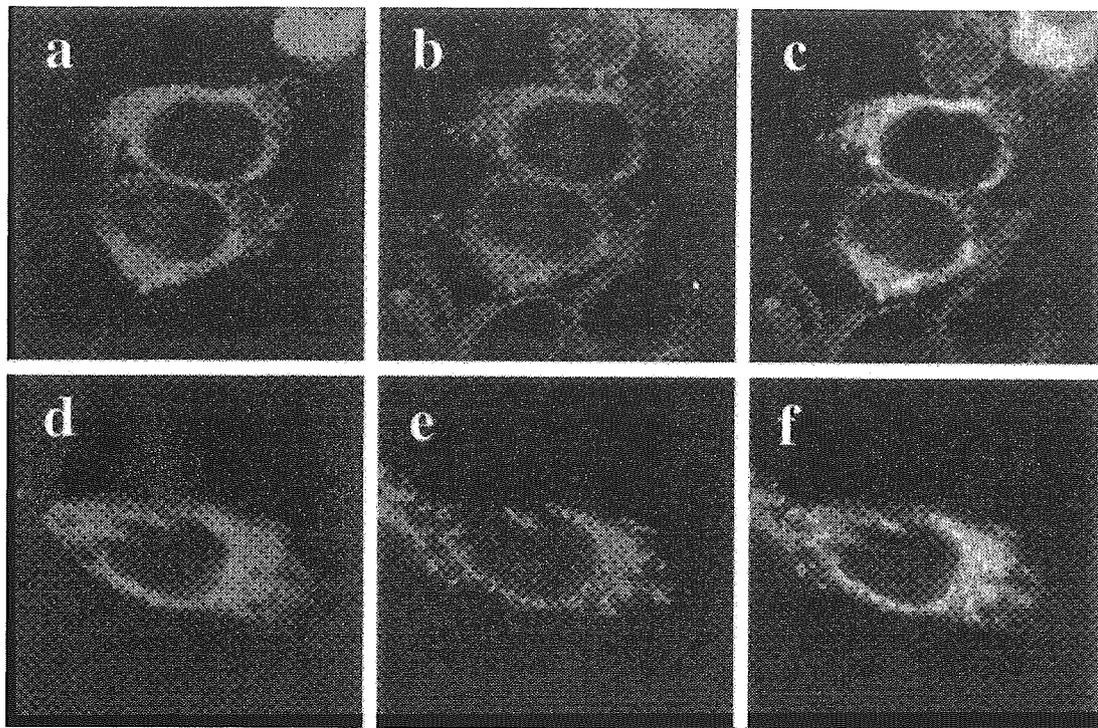
FIG. 1. Confocal analysis of double staining for HCV core protein and ER or mitochondria. 293T cells transfected with full-length HCV core expression plasmid, pCAGC191 were allowed to express the plasmid for 2 days. Transfected cells were fixed directly (a to c) or fixed after loading with Mitotracker (d to f). After permeabilization with Triton X-100, cells were subjected to immunofluorescence staining with a mouse anticore antibody. A goat anticalregulin antibody was used for ER staining. The green signals corresponding to the core were found with a fluorescein isothiocyanate-conjugated rabbit anti-mouse IgG (a and d). The red signals corresponding to the ER were obtained with a rhodamine-conjugated rabbit anti-goat IgG secondary antibody (b). Mitochondria were stained with the mitochondrion-selective dye Mitotracker (e). Overlay resulted in yellow signals indicative of colocalization (c and f).

cated on ice. GST and GST fusion proteins were purified from bacterial lysates with glutathione-Sepharose beads (Amersham Bioscience Corp.). The beads were washed four times with lysis buffer. Approximately equal amounts of purified protein, as estimated by Coomassie brilliant blue staining, were used for the binding assays. For pulldown assays, in vitro transcription and translation of importin-α was done with pRSET-hSRP1α and the TNT-coupled reticulocyte lysate system (Promega Corp., Madison, Wis.) with T7 RNA polymerase. The reaction was carried out at 30°C for 4 h in the presence of [^{35}S]methionine/cysteine (ICN Pharmaceuticals). The translation product was then incubated with glutathione-Sepharose beads bound to GST fusion proteins in 1 ml of binding buffer (40 mM HEPES [pH 7.5], 100 mM KCl, 0.1% NP-40, and 20 mM 2-mercaptoethanol) at 4°C for 1 h. The beads were washed four times with binding buffer, and the pulldown complexes were separated by SDS-PAGE on 15% polyacrylamide gels. The gels were then fixed, dried, and analyzed with autoradiography.

RESULTS

Subcellular localization of HCV core protein. To assess the subcellular localization of HCV core protein, we first analyzed cells transfected with a full-length core-expressing construct by confocal microscopy. In accordance with previous observations (2, 15, 32, 45, 56), a granular cytoplasmic staining pattern of the core protein was observed in 293T (Fig. 1) and human hepatoblastoma HepG2 (data not shown) cells. Dual staining of transfected cells with antibody against the ER protein calregulin along with anticore antibody confirmed the ER localization of the core protein (Fig. 1a, b, and c show the core,
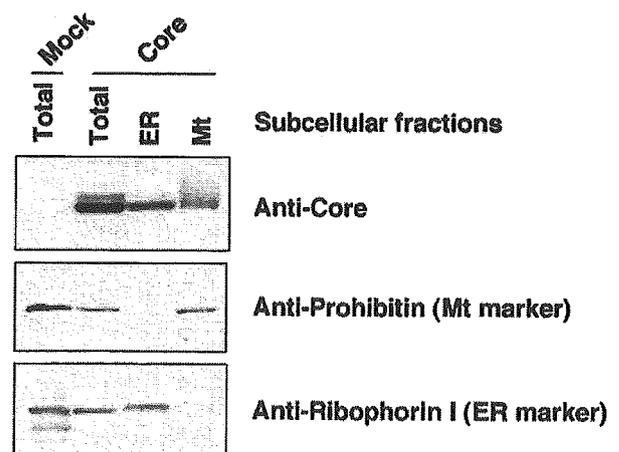

FIG. 2. Subcellular distribution of HCV core protein analyzed by immunoblotting. ER and mitochondrial (Mt) fractions were isolated from 293T cells expressing the full-length core protein (Core) or nontransfected cells (Mock) 2 days after transfection. Equal amounts of protein from each fraction as well as whole cell lysates (Total) were subjected to immunoblotting with a monoclonal antibody against either HCV core, prohibitin, or ribophorin I.
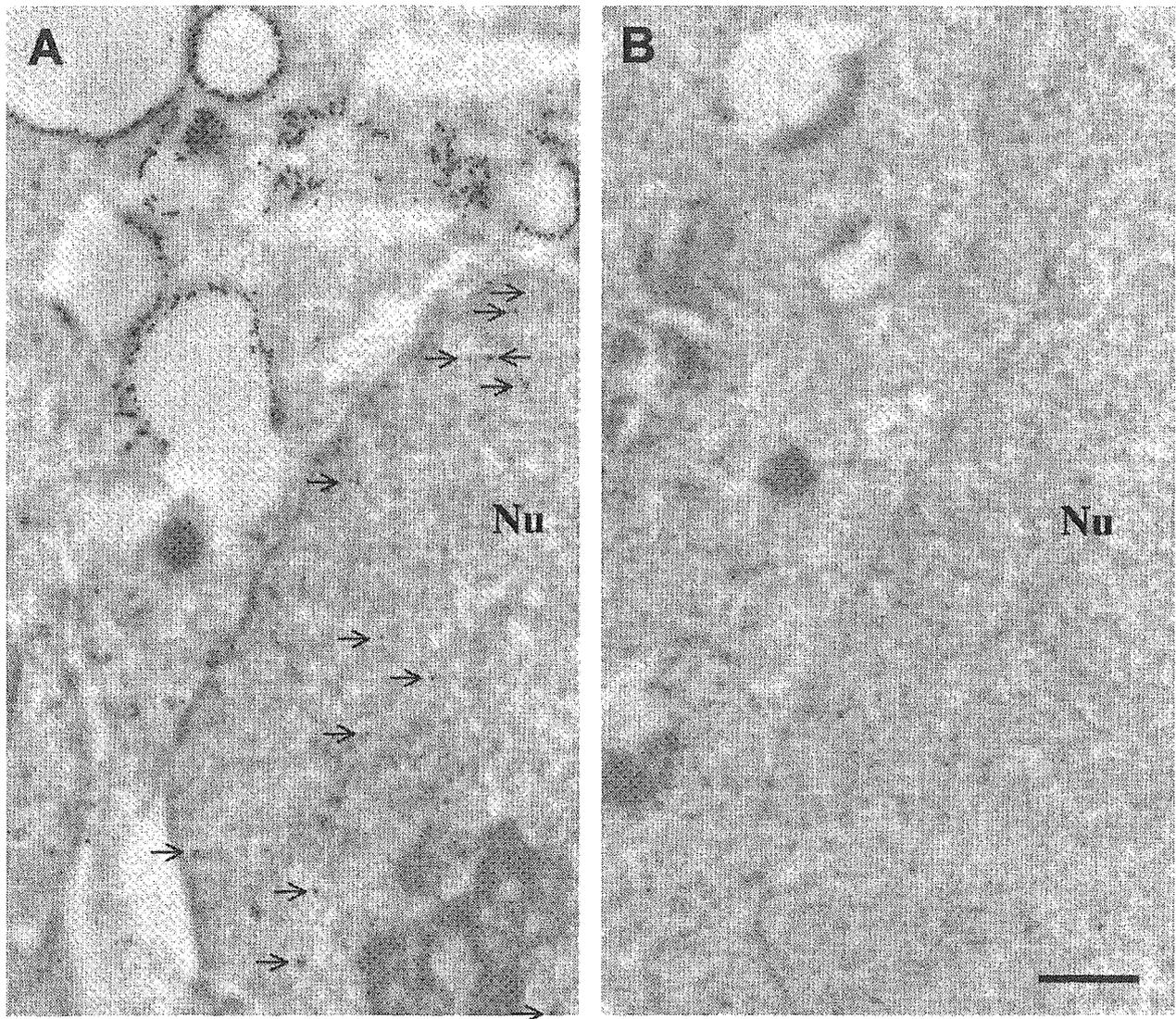
FIG. 3. Immunoelectron microscopy of HCV core protein. 293T cells expressing the full-length core protein (A) and nonexpressing cells (B) fixed 2 days after transfection. Immunoelectron microscopic analysis was performed with a mouse anticore antibody and a secondary anti-mouse IgG conjugated with gold particles. The arrows indicate the core protein localized in the nucleus (Nu). Bar, 500 nm.

calregulin, and a merged image, respectively). The pattern of subcellular localization of the core protein (Fig. 1d) was compared to the distribution of mitochondria, as revealed by MitoTracker staining (Fig. 1e). Although distribution of the core protein was not completely identical with that of the mitochondrion-selective dye, overlapping staining was observed, particularly in the perinuclear region (Fig. 1f).

Intracellular localization of the core protein was further examined in 293T cells by subcellular fractionation and Western blotting. The core protein was present in both the ER and mitochondrial fractions (Fig. 2), while it was not detected in the cytosol fraction (data not shown). The purity of the ER and mitochondrial fractions was confirmed with antibodies against ribophorin I as an ER marker and prohibitin as a mitochondrial marker.

It is generally difficult to identify the nuclear distribution of proteins of interest due to contamination of the nuclear preparation with unbroken, intact cells. Thus, to investigate whether the core protein localizes to the nucleus, we examined transfected cells by immunoelectron microscopy. Although gold particles were primarily observed within cytoplasmic membranes, perhaps highlighting the ER, immunoreactivity to anticore antibody was also observed in the nucleus (Fig. 3A, arrows). In contrast, no antibody labeling was observed in cells transfected with an empty vector (Fig. 3B).

Thus, HCV core protein predominates in the cytoplasm in a membrane-associated form(s) with ER and mitochondria, but nuclear localization is also observed.

Regions responsible for directing core protein to the ER and mitochondria. Given the tendency of the core protein to lo-
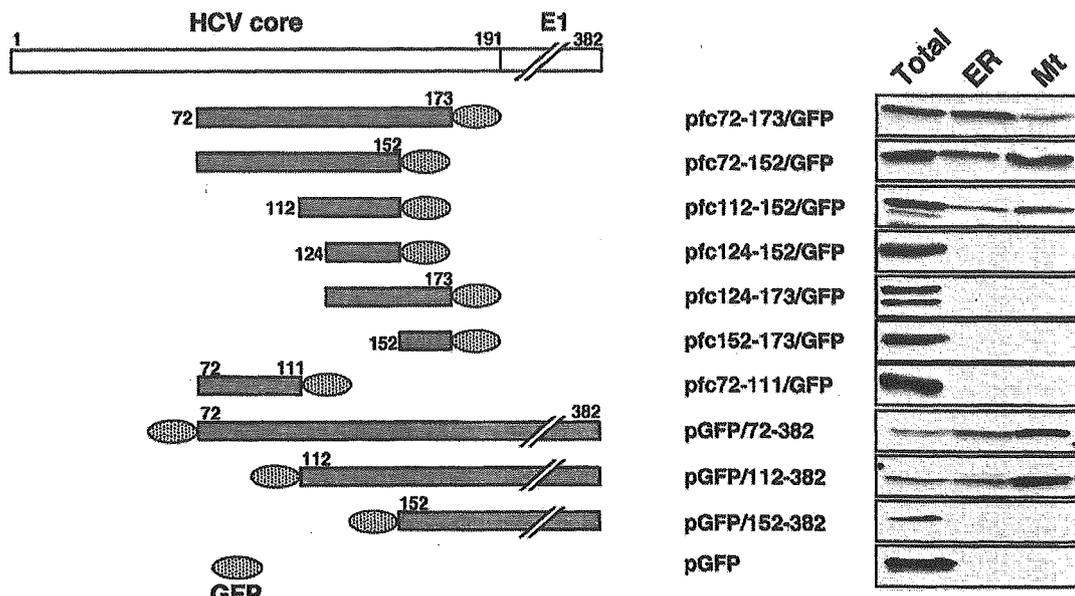
FIG. 4. Identification of segments that mediate association with ER and mitochondria in the core protein. Schematic diagram (left) and nomenclature (middle) of the core-GFP fusions are shown. Gray bars, expressed core and E1 regions. Subcellular distribution of fusion proteins is indicated on the right. ER and mitochondrial (Mt) fractions as well as whole-cell lysates (Total) were subjected to immunoblotting with an anti-GFP antibody.

calize to the ER and to mitochondria, we next investigated whether specific sequences might be responsible for transporting the core protein to these organelles. Fusion proteins between different regions of the core protein and GFP were developed, with specific emphasis on the region downstream of amino acid 72 because this region contains clusters of hydrophobic amino acids and the N-terminal 71 residues of the core are known to play a role in nuclear targeting (6, 48).

Western blotting of subcellular fractions with anti-GFP antibody revealed the localization of a core (72–173)-GFP fusion protein to the ER and to mitochondria (Fig. 4). Fusion proteins containing GFP and core proteins with N- or C-terminal deletions (72-152-GFP and 112-152-GFP) were likewise identified within the ER and mitochondrial fractions. In contrast, the ER and mitochondrial fractions did not contain GFP fusion proteins containing core protein amino acids 124 to 152, 124 to 173, 152 to 173, or 72 to 111. These fusion proteins demonstrated distribution profiles similar to that of GFP alone. We also tested GFP-core-E1 fusions, which are processed at the C terminus of the core by signal peptidase and signal peptide peptidase (19, 30). GFP-core fusions expressed from pGFP/72–382 and pGFP/112–382 were detected in the ER and mitochondrial fractions. The fusion expressed from pGFP/152–382 was not identified in these fractions.

We further analyzed subcellular localization of the fusion proteins by confocal immunofluorescence microscopy (Fig. 5). As expected, fusions of (72–173)-GFP and (112–152)-GFP exhibited localization to the ER and mitochondria. The patterns of subcellular localization of these fusions are indistinguishable from that of the full-length core protein, as shown in Fig. 1. Expression of (124–152)-GFP or (112–123)-GFP resulted in widespread diffusion of the fusion in the cell. Thus, these

results indicate that the region spanning amino acids 112 to 152 can mediate association of the core protein not only to the ER but also to the mitochondria.

We subsequently examined the submitochondrial localization of the core protein with a protease protection assay. As shown in Fig. 6A, HCV core protein localized in the mitochondria was completely digested upon treatment with proteinase K for 30 min at 0°C. Under identical conditions, a marker specific for the mitochondrial outer membrane, Tom20, was also observed to disappear, whereas digestion of a mitochondrial inner membrane marker, Tim17, was not observed. These findings confirm that HCV core protein is localized to the mitochondrial outer membrane.

The predicted secondary structure of the region, amino acids 72 to 173, is shown in Fig. 6B. The presence of a long helical segment, lying between amino acids 116 and 134, and two short α-helices (amino acids 146 to 152 and amino acids 155 to 159) were predicted. The results of the cell fractionation assay and confocal microscopy with a series of deletion mutants shown in Fig. 4 and 5 suggest that an α-helix between amino acids 116 and 134 may be required for associating the core protein with the ER and the mitochondrial outer membrane. When amino acids 117 to 134 are portrayed as a helical wheel, we found an amphipathic structure with hydrophobic residues on one side and polar residues on the other side of the α-helix (Fig. 6C), which is often observed in membrane-associated proteins. This helical conformation might be important for directing the core protein to the ER and mitochondrial outer membranes.

Nuclear localization of the HCV core protein is mediated by a bipartite NLS, possibly via an importin-dependent pathway. Although HCV core protein is mainly localized within the cytoplasm, it is also found in the nucleus, as shown in Fig. 3.
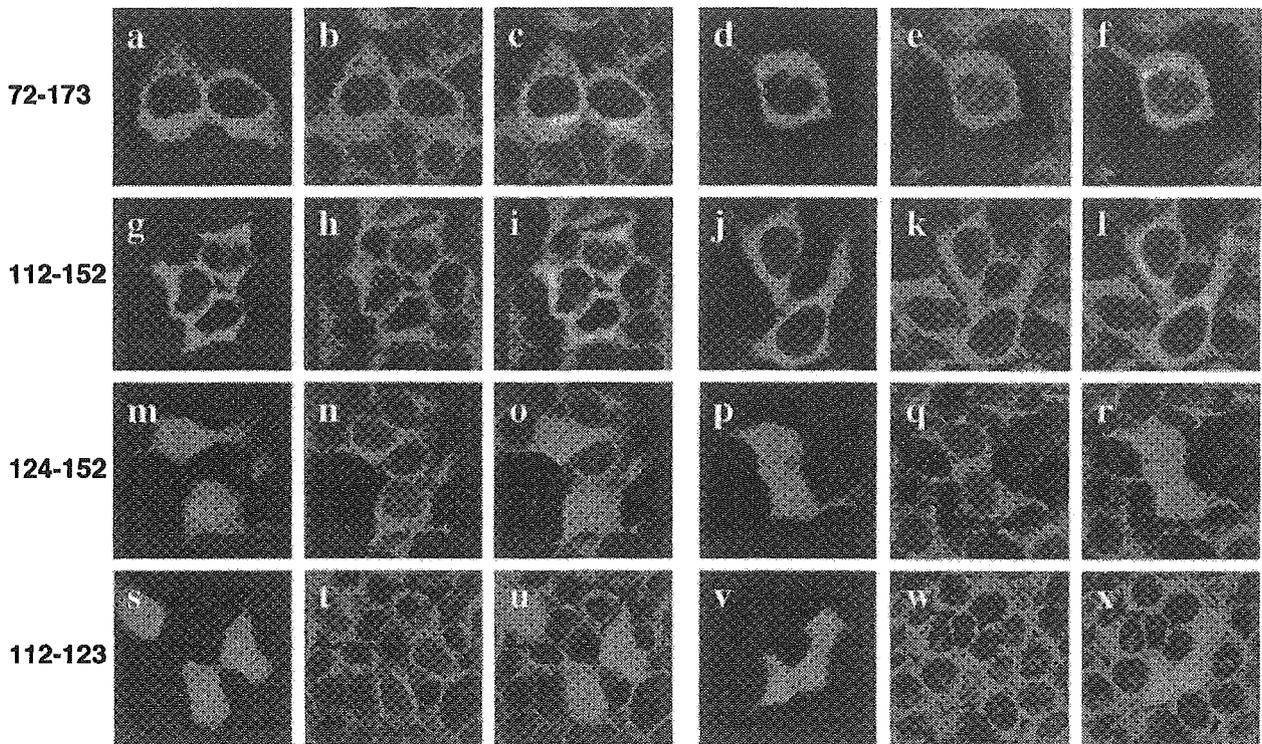
FIG. 5. Confocal analysis of double staining for core-GFP fusion protein and ER or mitochondria. 293T cells transfected with core-GFP expression plasmids (72–173, 112–152, 124–152, and 112–123) were allowed to express the plasmid for 2 days. Transfected cells were fixed directly (a to c, g to i, m to o, and s to u) or fixed after loading with Mitotracker (d to f, j to l, p to r, and v to x). After permeabilization with Triton X-100, a goat anticalregulin antibody was used for ER staining. The red signals corresponding to the ER were obtained with a rhodamine-conjugated rabbit anti-goat IgG secondary antibody (b, h, n, and t). Mitochondria were stained with the mitochondrion-selective dye Mitotracker (e, k, q, and w). Overlay resulted in yellow signals indicative of colocalization (c, f, i, l, o, r, u, and x).

The results of previous studies demonstrate that the N-terminal region of the core protein is responsible for nuclear targeting. It contains three clusters of basic amino acid residues that represent putative consensus motifs for NLS sequences PKPQRKTKR (amino acids 5 to 13), PRRGPR (amino acids 38 to 43), and PRGRRQPIPKARRP (amino acids 58 to 71) (6, 48). Nuclear targeting is generally governed by a family of transporters or cytosolic receptor proteins, known as importins or karyopherins, which function in concert with a guanine nucleotide-binding protein named Ran and other regulatory proteins such as NTF2/p10. Conventional NLS-dependent nuclear targeting occurs when importin-α recognizes the NLS sequence, mediating binding to importin-β1, after which the trimeric complex translocates to the nucleus (12).

In order to determine whether the putative NLS motifs identified within the core protein sequence are capable of binding to importin-α, we examined the in vitro interaction between bacterially expressed GST-fused core protein and ^{35}S-labeled importin-α with a GST pulldown assay. We then substituted lysine and arginine residues of one or more of the putative NLS motifs of the core protein (all contained within the first 71 amino acids of the N terminus) with alanine and fused the resultant constructs with GST, as shown schematically in Fig. 7A. As shown in Fig. 7B (upper panel), importin-α was pulled down by a GST fusion protein containing wild-type core (amino acids 1 to 71) protein but not with GST alone,

suggesting that direct binding occurs between the core protein and importin-α. Importin-α was also pulled down by GST-core fusion proteins containing substitutions in one or two NLS motifs (NLS/m1, NLS/m2, NLS/m3, NLS/m4, NLS/m5, and NLS/m6). However, importin-α was not pulled down by GST-core fusion proteins containing alanine substitutions in all three NLS motifs (NLS/m7). It should be noted that similar amounts of GST fusion proteins were used for each of the in vitro pulldown assays, followed by SDS-PAGE and Coomassie brilliant blue staining (Fig. 7B, lower panel). These results demonstrated that all three putative NLS motifs of the N-terminal region of the core protein can mediate binding to importin-α, which suggests that nuclear translocation of the core protein occurs via an importin-dependent pathway (12).

The interaction between the core and importin-α was further analyzed by a colocalization assay (Fig. 7C). The GFP fusion containing the wild-type core (amino acids 1 to 71) was well colocalized with HA-importin-α; distribution of the two proteins showed similar nuclear staining patterns, confirming the presence of a functional NLS sequence(s) within the core protein. In contrast, NLS/m4, with substitutions in two NLS motifs, was partly colocalized with HA-importin-α near or around the nuclear membrane, suggesting that NLS motif double mutants bind to importin-α but their binding efficiency is lower than that of wild-type core protein.

Finally, we examined the subcellular localization of core

A   -   + (Proteinase K)   **B**

Anti-Core

Anti-Tom20

Anti-Tim17

```
72                                                                      116
EGRTWAQPGYPWPLYGNEGLGWAGWLLSPRGSRPSWGPNDPRRRSRNLGKV
tt       tt              tt    eeeeee              HHHHHHH
           134                                                    173
IDTLTCGFADLMGYIPLVGAPLGGAARALAHGVRVLEDGVNYATGNLPGCS
HHHHHHHHHHHHHHteeeee        tHHHHHHHttHHHHHHtt   eett
```
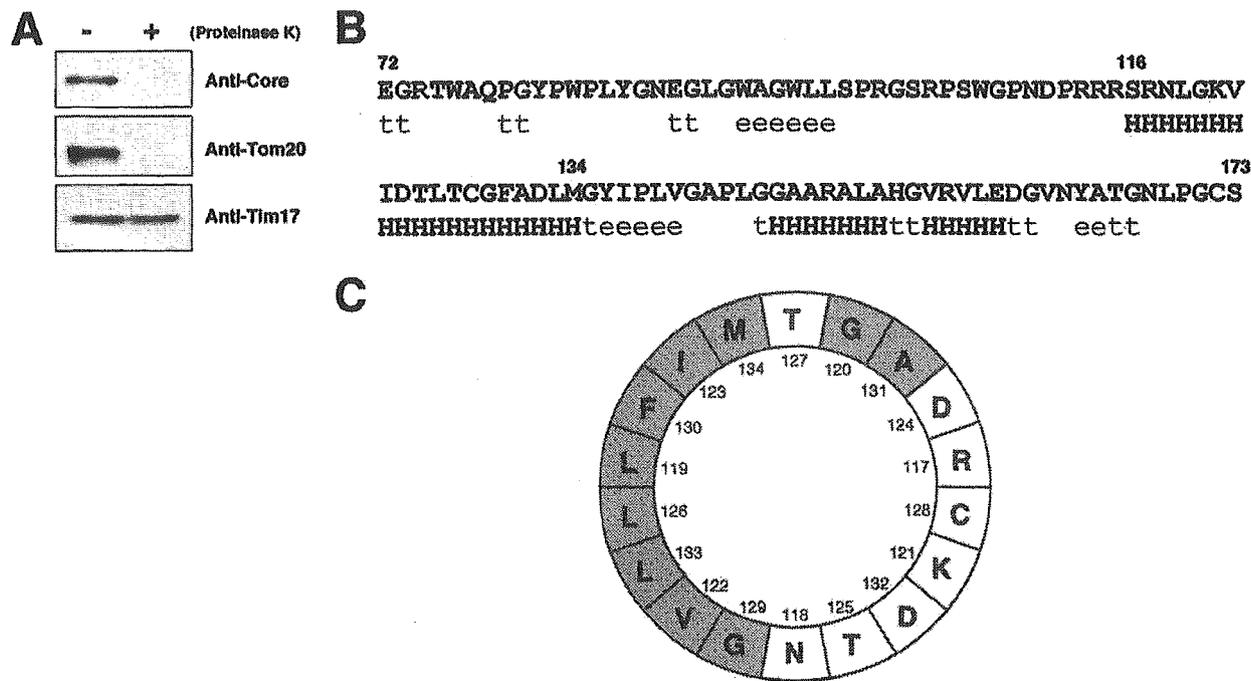
C

FIG. 6. (A) Protease protection assay. A mitochondrial fraction isolated from cells expressing the core protein was treated with proteinase K (+) as described in Materials and methods. The sample as well as the nontreated fraction (−) were subjected to immunoblotting with a monoclonal antibody against either HCV core, Tom20, or Tim17. (B) Protein sequence and predicted secondary structure of HCV core, amino acids 72 to 173. The secondary structure prediction was obtained with the self-optimized prediction method, a computer program on the internet (http://npsa-pbil .ibcp.fr/cgi-bin/npsa_automat.pl?page = /NPSA/npsa_sopm.html). H, α-helix; t, turn; e, extension. (C) α-Helical plot of amino acids 117 to 134 of the core protein. In the helical wheel plots, the gray shading represents apolar and hydrophobic residues; and the white represents polar residues.

protein expressed by the wild-type and NLS mutants (Fig. 7D). As expected, a fusion protein containing wild-type core protein (amino acids 1 to 71) and GFP was localized exclusively to the nucleus. Core proteins from three fusion proteins containing substitutions in each NLS motif (NLS/m1, NLS/m2, and NLS/m3) were detected primarily in the nucleus. Weak fluorescence was also observed in the cytoplasm, suggesting that these mutations caused a slight reduction in the efficiency of nuclear translocation. On the other hand, two or three NLS motif substitution mutations (NLS/m4, NLS/m5, NLS/m6, and NLS/m7) completely abolished nuclear translocation, resulting in a diffuse distribution of core protein, similar to that of GFP alone. Although it is likely that all three putative NLS motifs play a role, the above results suggest that at least two of the three putative NLS motifs are prerequisite for efficient nuclear translocation of the core protein.

DISCUSSION

HCV core protein is released from the viral polyprotein by a host protease(s) within the ER membrane at a signal peptide sequence lying between the core and envelope (E1) proteins (16, 41). Subsequently, the signal peptide is further processed by an intramembranous protease called signal peptide peptidase (38, 53). This mature form of the core protein is then released and undergoes subcellular trafficking (30, 53). The core protein localizes mainly to the ER, mitochondria, and

lipid droplets. Some reports also describe localization of the core protein to the nuclei of hepatocytes in HCV-infected patients (10), transgenic mice (34), and cultured cells expressing viral polyproteins (56). Although it has been reported which sequence motifs are responsible for localization of the HCV core protein to lipid droplets and nuclei, it is uncertain which sequences target the core protein to the ER and to mitochondria. In this study, we identified sequences related to localization of the mature core protein to the ER and to mitochondria.

Through heterologous expression of core-GFP fusion proteins containing a series of deletions, we determined that a sequence extending from amino acids 112 to 152 of the core protein is required for its localization at the mitochondrial outer membrane. Translocation of nucleus-encoded mitochondrial proteins is usually dependent on N-terminal sequences, referred to as mitochondrial targeting sequences (37). However, it is also true that a significant proportion of mitochondrial proteins lack these N-terminal mitochondrial targeting sequences. Specifically, a number of outer membrane proteins do not have cleavable sequences at their N termini; rather, they are targeted to mitochondria by means of internal or C-terminal signals (31).

Since it has been reported that amino acid sequences required for targeting to the outer mitochondrial membrane form a highly hydrophobic α-helical wheel, as seen in A-kinase associated protein 84/12 (4) and NADH-cytochrome *b* reduc-
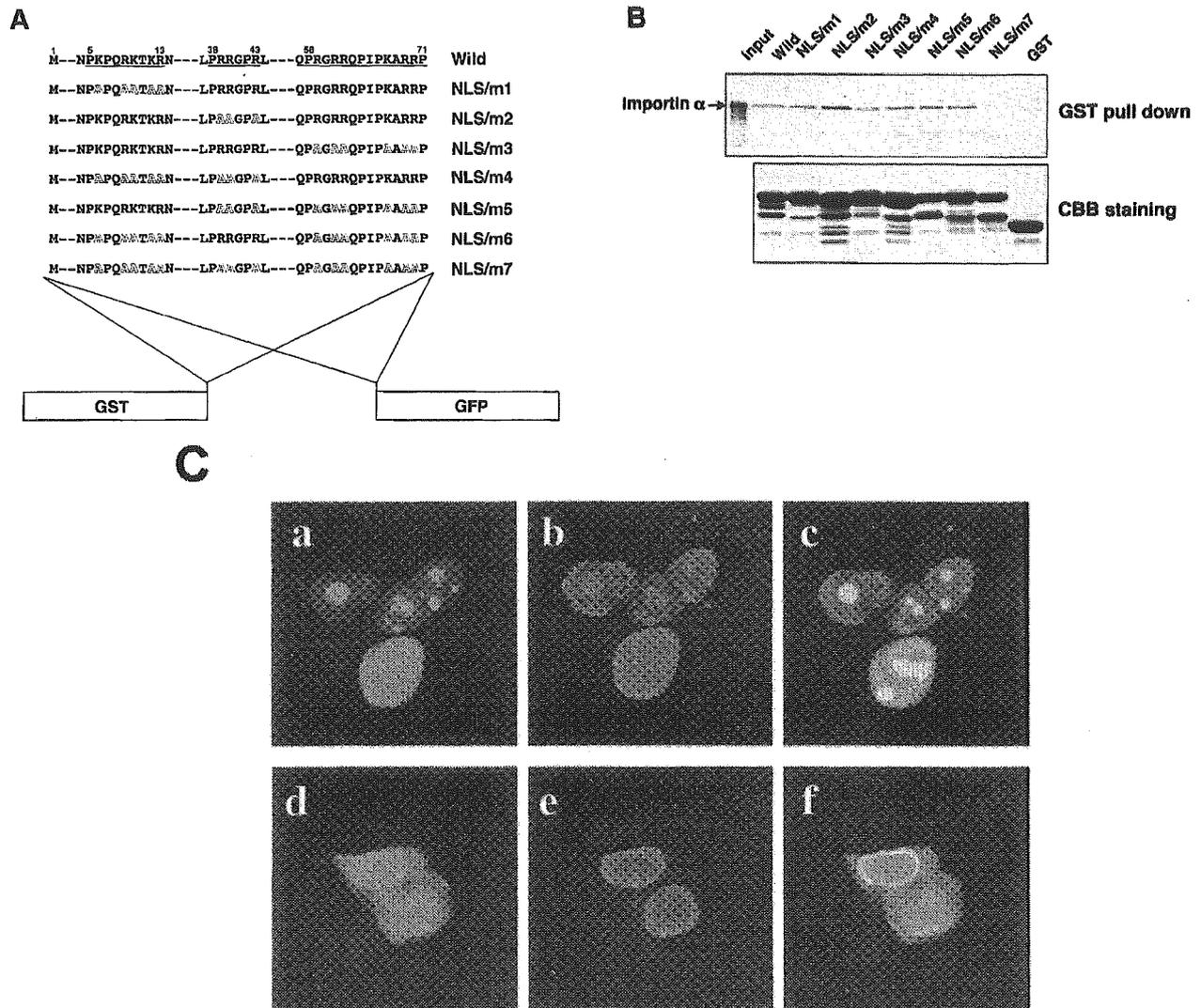
A

```
  1    5        13        38   43        58         71
M--NPKPQRKTKRN---LPRRGPRL---QPRGRRQPIPKARRP    Wild
M--NPSPQSRTSRN---LPRRGPRL---QPRGRRQPIPKARRP   NLS/m1
M--NPKPQRKTKRN---LPRRGPRL---QPRGRRQPIPKARRP   NLS/m2
M--NPKPQRKTKRN---LPRRGPRL---QPRGRRQPIPKARRP   NLS/m3
M--NPSPQRRTRRN---LPRRGPRL---QPRGRRQPIPKARRP   NLS/m4
M--NPKPQRKTKRN---LPRRGPRL---QPRGRRQPIPKARRP   NLS/m5
M--NPSPQRRTRRN---LPRRGPRL---QPRGRRQPIPKARRP   NLS/m6
M--NPSPQRRTRRN---LPRRGPRL---QPRGRRQPIPKARRP   NLS/m7
```

GST   GFP

B

Importin α→

GST pull down

CBB staining

C

a   b   c
d   e   f

FIG. 7. Mutational analyses of NLS motifs in HCV core protein. (A) Schematic structures of fusion proteins and amino acid sequences corresponding to putative NLS motifs, three basic clusters (underlined) in the core protein. Two series of constructs fused with either GFP or GST were created. The mutated basic residues are indicated with outline letters. (B) GST pulldown assay. Equal amounts of GST fusions as described in A or GST alone was immobilized on glutathione-Sepharose 4B beads and incubated with in vitro-translated, [^{35}S]methionine-labeled importin-α. Bound material was separated by SDS-PAGE, and the amount of importin-α bound was detected by autoradiography. Direct electrophoretic separation of in vitro translation products served as a control (input). Coomassie brilliant blue staining of GST fusions and GST alone are shown in the bottom panel. (C) Confocal analysis of double staining for core-GFP fusion protein and HA-importin-α. 293T cells transfected with the wild-type core (1–71)-GFP (a to c) or NLS/m4 (d to f) expression plasmid and pCAG-HA-imp were allowed to express for 2 days. After the cells were fixed and permeabilized, they were incubated with a mouse anti-HA antibody. The red signals corresponding to HA-importin-α were obtained with a rhodamine-conjugated goat anti-mouse IgG secondary antibody (b and e). Overlay resulted in yellow signals indicative of colocalization (c and f). (D) Subcellular localization of GFP fusion proteins. GFP fusions with and without substitution mutations in the NLS motifs of the core protein as described in A were expressed in 293T cells. GFP images of the fixed cells were recorded.

tase (14), a predicted structure of an amphipathic α-helix present between amino acids 116 and 134 (Fig. 6B and C) possibly plays a role in directing the core protein to the mitochondrial outer membrane. Sequence comparisons demonstrate conservation of the amino acid sequence and secondary structure of the region, amino acids 112 to 152, among a variety of HCV isolates, including the infectious H77c clone (55), as well as a full-length adaptive replicon (3). To gain insight into

the significance of the secondary structure of the region in targeting to the mitochondria, further structural and biochemical analyses are needed.

The association of HCV core protein with the mitochondrial membrane suggests that the core protein has the ability to modulate mitochondrial function, possibly by altering the permeability of the mitochondrial membrane. The core protein induces the production of cellular reactive oxygen species in
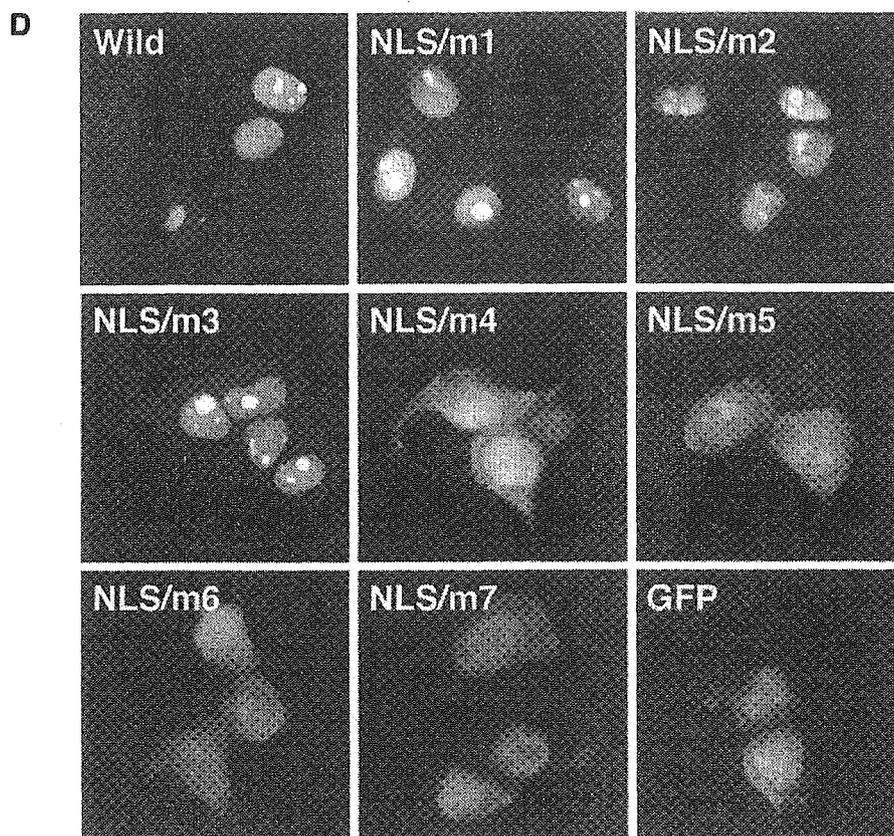
D

FIG. 7—*Continued.*

the livers of core-transgenic mice and in core-expressing cell lines (35). Reactive oxygen species, predominantly generated in mitochondria, induce genetic mutations and act as secondary messengers to regulate a variety of cellular functions, including gene expression and proliferation (1). Although the molecular mechanism by which core protein induces reactive oxygen species production is still unclear, HCV core protein is known to impair the mitochondrial electron transfer system (35). The core protein may also modulate apoptosis, since mitochondria play a major role in regulating programmed cell death. Expression of HCV proteins, including the core protein, suppresses the release of cytochrome *c* from mitochondria to the cytoplasm in HCV-transgenic mice, thus inhibiting Fas-mediated apoptosis (27).

Okamoto et al. recently reported that not only the C-terminal signal sequence but also amino acids 128 to 151 are required for ER retention of the core protein by using a series of N-terminally truncated core protein constructs (38). Here, in this study, we further showed that amino acids 112 to 152 mediate association of the core protein with the ER in the absence of the C-terminal signal sequence. Hope and McLauchlan demonstrated that the central domain of the core protein, amino acids 119 to 174, is important for association with lipid droplets (17). They also showed that this corresponding domain is shared with GB virus B, which is most closely related to HCV, but not with either pestiviruses or flaviviruses

(18). It appears that the 41 residues identified as the sequence mediating association with the ER membrane in the present study are crucial for directing the core protein to lipid droplets, since the surface of lipid droplets must derive from the cytoplasmic side of the ER membrane.

The HCV core protein contains NLS sequences which are composed of three stretches of sequences rich in basic residues. These sequences were originally identified by experiments with fused forms of wild-type and mutated core proteins with β-galactosidase (6, 48). C-terminally truncated versions of the core protein localize exclusively to the nucleus (48). A fraction of the core protein is detected in the nucleus even when full-length HCV core gene is expressed (Fig. 2) and as described (34, 56). However, it is difficult to demonstrate clearly the nuclear localization of the core protein by immunofluorescence, presumably because of the instability of nuclearly localized core protein (49, 33). We only observed a nuclear staining pattern of the matured core protein after adding proteasome inhibitors to the culture (33).

Generally, NLS sequences fall into two categories; (i) monopartite NLSs, which contain a single cluster of basic residues, and (ii) bipartite NLSs, which contain two clusters of basic residues separated by an unconserved linker sequence of variable length (reviewed in reference 12). Nuclear translocation of an NLS-containing cargo protein is initiated when the soluble import receptor (importin) recognizes the NLS-contain-

ing protein within the cytoplasm. Importin-α contains an NLS-binding site(s), and importin-β docks importin-cargo complexes to the cytoplasmic filaments of a nuclear pore complex, after which translocation occurs through the nuclear pore. Thus, importin-α functions as an adaptor between the bona fide import receptor and the NLS-containing protein.

We further characterized the NLS of the core protein and found that each of the NLS motifs of the core protein is able to bind to importin-α and that at least two NLS motifs are required for efficient nuclear distribution of the core protein in cells. It appears that double mutations among three NLS motifs decrease the ability of the core protein to bind importin-α. These observations suggest that the binding of the double mutants with importin-α leads to no or little active translocation of the core protein into the nucleus. The double mutations may also block subsequent interactions with importin-β1, GTPase Ran, and/or NTF2/p10, which are required for translocation through the nuclear pore complexes.

The findings obtained in this study suggest that HCV core protein NLS motifs have a bipartite function. Crystallographic studies of monopartite (e.g., simian virus 40 large T antigen) and bipartite (e.g., nucleoplasmin) NLSs show that the basic residue clusters of bipartite NLSs occupy separate binding sites on importin-α. In contrast, while monopartite NLSs can bind to the same sites as bipartate NLSs on importin-α, they mainly bind to the N-terminal binding site, which is referred to as the major binding site on importin-α (9, 11). A recent report describes an importin-α variant with a mutation in the major site which results in decreased ability to bind both monopartite and bipartite NLSs. Another variant with a mutation in the minor site exhibits decreased binding only to bipartite NLS-containing proteins, making importin-α nonfunctional in vivo (22). Thus, we favor a model in which the core protein bipartite NLS, composed of any two of the three basic clusters, occupies both major and minor binding sites on importin-α, resulting in efficient nuclear translocation. Importin-α may be equally accessible to all clusters, given their close proximity to one another, as well as the distinct conformational flexibility of the ≈70-residue N-terminal region of the core protein.

With regard to the molecular mechanisms participating in nuclear localization of the core protein, Moriishi et al. found that PA28γ is involved in nuclear localization of the core protein. Interaction of the core protein with PA28γ plays an important role in retention of the core protein in the nucleus (33). Furthermore, in yeast cells, nuclear transport of the core protein requires the activity of the small GTPase Ran/Gsp1p and is mediated by Kap123p, but neither importin-α nor importin-β is involved (20). Differences in nucleocytoplasmic transport between yeast and mammalian cells might explain the inconsistencies observed in the present study. Further experiments are required to characterize the exact nature of the interaction between the core protein and components of the nuclear import machinery, particularly in cells where HCV is replicating.

In conclusion, the mature HCV core protein has an internal 41-amino-acid sequence mediating association of the viral protein with the ER and mitochondria. We also provide evidence for a novel class of bipartite NLS contained within the core protein, which comprises two of three basic motifs, thus enabling efficient nuclear targeting. Multiple functional domains

influence the subcellular localization of the core protein, which ultimately depends on the balance of the respective signals.

REFERENCES

1. Adler, V., Z. Yin, K. D. Tew, and Z. Ronai. 1999. Role of redox potential and reactive oxygen species in stress signaling. Oncogene 18:6104–6111.
2. Barba, G., F. Harper, T. Harada, M. Kohara, S. Goulinet, Y. Matsuura, G. Eder, Z. Schaff, M. J. Chapman, T. Miyamura, and C. Bréchot. 1997. Hepatitis C virus core protein shows a cytoplasmic localization and associates to cellular lipid storage droplets. Proc. Natl. Acad. Sci. USA 94:1200–1205.
3. Bukh, J., T. Pietschmann, V. Lohmann, N. Krieger, K. Faulk, R. E. Engle, S. Govindarajan, M. Shapiro, M. St Claire, and R. Bartenschlager. 2002. Mutations that permit efficient replication of hepatitis C virus in Huh-7 cells prevent productive replication in chimpanzees. Proc. Natl. Acad. Sci. USA 99:14416–14421.
4. Cardone, L., T. de Cristofaro, A. Affaitati, C. Garbi, M. D. Ginsberg, M. Saviano, S. Varrone, C. S. Rubin, M. E. Gottesman, E. V. Avvedimento, and A. Feliciello. 2002. A-kinase anchor protein 84/121 are targeted to mitochondria and mitotic spindles by overlapping amino-terminal motifs. J. Mol. Biol. 320:663–675.
5. Chang, J., S. H. Yang, Y. G. Cho, S. B. Hwang, Y. S. Hahn, and Y. C. Sung. 1998. Hepatitis C virus core from two different genotypes has an oncogenic potential but is not sufficient for transforming primary rat embryo fibroblasts in cooperation with the H-ras oncogene. J. Virol. 72:3060–3065.
6. Chang, S. C., J. H. Yen, H. Y. Kang, M. H. Jang, and M. F. Chang. 1994. Nuclear localization signals in the core protein of hepatitis C virus. Biochem. Biophys. Res. Commun. 205:1284–1290.
7. Choo, Q. L., G. Kuo, A. J. Weiner, L. R. Overby, D. W. Bradley, and M. Houghton. 1989. Isolation of a cDNA clone derived from a blood-borne non-A, non-B viral hepatitis genome. Science 244:359–362.
8. Choo, Q. L., K. H. Richman, J. H. Han, K. Berger, C. Lee, C. Dong, C. Gallegos, D. Coit, R. Medina-Selby, P. J. Barr, et al. 1991. Genetic organization and diversity of the hepatitis C virus. Proc. Natl. Acad. Sci. USA 88:2451–2455.
9. Conti, E., M. Uy, L. Leighton, G. Blobel, and J. Kuriyan. 1998. Crystallographic analysis of the recognition of a nuclear localization signal by the nuclear import factor karyopherin alpha. Cell 94:193–204.
10. Falcon, V., N. Acosta-Rivero, G. Chinea, M. C. de la Rosa, I. Menendez, S. Duenas-Carrera, B. Gra, A. Rodriguez, V. Tsutsumi, M. Shibayama, J. Luna-Munoz, M. M. Miranda-Sanchez, J. Morales-Grillo, and J. Kouri. 2003. Nuclear localization of nucleocapsid-like particles and HCV core protein in hepatocytes of a chronically HCV-infected patient. Biochem. Biophys. Res. Commun. 310:54–58.
11. Fontes, M. R., T. Teh, and B. Kobe. 2000. Structural basis of recognition of monopartite and bipartite nuclear localization sequences by mammalian importin-alpha. J. Mol. Biol. 297:1183–1194.
12. Görlich, D., and U. Kutay. 1999. Transport between the cell nucleus and the cytoplasm. Annu. Rev. Cell. Dev. Biol. 15:607–660.
13. Grakoui, A., D. W. McCourt, C. Wychowski, S. M. Feinstone, and C. M. Rice. 1993. Characterization of the hepatitis C virus-encoded serine proteinase: determination of proteinase-dependent polyprotein cleavage sites. J. Virol. 67:2832–2843.
14. Hahne, K., V. Haucke, L. Ramage, and G. Schatz. 1994. Incomplete arrest in the outer membrane sorts NADH-cytochrome b5 reductase to two different submitochondrial compartments. Cell 79:829–839.
15. Harada, S., Y. Watanabe, K. Takeuchi, T. Suzuki, T. Katayama, Y. Takebe, I. Saito, and T. Miyamura. 1991. Expression of processed core protein of hepatitis C virus in mammalian cells. J. Virol. 65:3015–3021.
16. Hijikata, M., N. Kato, Y. Ootsuyama, M. Nakagawa, and K. Shimotohno. 1991. Gene mapping of the putative structural region of the hepatitis C virus

genome by in vitro processing analysis. Proc. Natl. Acad. Sci. USA **88:**5547–5551.

17. **Hope, R. G., and J. McLauchlan.** 2000. Sequence motifs required for lipid droplet association and protein stability are unique to the hepatitis C virus core protein. J. Gen. Virol. **81:**1913–1925.

18. **Hope, R. G., D. J. Murphy, and J. McLauchlan.** 2002. The domains required to direct core proteins of hepatitis C virus and GB virus-B to lipid droplets share common features with plant oleosin proteins. J. Biol. Chem. **277:**4261–4270.

19. **Hüssy, P., H. Langen, J. Mous, and H. Jacobsen.** 1996. Hepatitis C virus core protein: carboxy-terminal boundaries of two processed species suggest cleavage by a signal peptide peptidase. Virology **224:**93–104.

20. **Isoyama, T., S. Kuge, and A. Nomoto.** 2002. The core protein of hepatitis C virus is imported into the nucleus by transport receptor Kap123p but inhibits Kap121p-dependent nuclear import of yeast AP1-like transcription factor in yeast cells. J. Biol. Chem. **277:**39634–39641.

21. **Lai, M. M., and C. F. Ware.** 2000. Hepatitis C virus core protein: possible roles in viral pathogenesis. Curr. Top. Microbiol. Immunol. **242:**117–134.

22. **Leung, S. W., M. T. Harreman, M. R. Hodel, A. E. Hodel, and A. H. Corbett.** 2003. Dissection of the karyopherin alpha nuclear localization signal (NLS)-binding groove: functional requirements for NLS binding. J. Biol. Chem. **278:**41947–41953.

23. **Liu, Q., C. Tackney, R. A. Bhat, A. M. Prince, and P. Zhang.** 1997. Regulated processing of hepatitis C virus core protein is linked to subcellular localization. J. Virol. **71:**657–662.

24. **Lo, S. Y., F. Masiarz, S. B. Hwang, M. M. Lai, and J. H. Ou.** 1995. Differential subcellular localization of hepatitis C virus core gene products. Virology **213:**455–461.

25. **Lo, S. Y., M. Selby, M. Tong, and J. H. Ou.** 1994. Comparative studies of the core gene products of two different hepatitis C virus isolates: two alternative forms determined by a single amino acid substitution. Virology **199:**124–131.

26. **Lu, W., A. Strohecker, and J. H. Ou.** 2001. Post-translational modification of the hepatitis C virus core protein by tissue transglutaminase. J. Biol. Chem. **276:**47993–47999.

27. **Machida, K., K. Tsukiyama-Kohara, E. Seike, S. Tone, F. Shibasaki, M. Shimizu, H. Takahashi, Y. Hayashi, N. Funata, C. Taya, H. Yonekawa, and M. Kohara.** 2001. Inhibition of cytochrome c release in Fas-mediated signaling pathway in transgenic mice induced to express hepatitis C viral proteins. J. Biol. Chem. **276:**12140–12146.

28. **Matsumoto, M., S. B. Hwang, K. S. Jeng, N. Zhu, and M. M. Lai.** 1996. Homotypic interaction and multimerization of hepatitis C virus core protein. Virology **218:**43–51.

29. **McLauchlan, J.** 2000. Properties of the hepatitis C virus core protein: a structural protein that modulates cellular processes. J. Viral Hepatitis **7:**2–14.

30. **McLauchlan, J., M. K. Lemberg, G. Hope, and B. Martoglio.** 2002. Intramembrane proteolysis promotes trafficking of hepatitis C virus core protein to lipid droplets. EMBO J. **21:**3980–3988.

31. **Mihara, K.** 2000. Targeting and insertion of nuclear-encoded preproteins into the mitochondrial outer membrane. Bioessays **22:**364–371.

32. **Moradpour, D., C. Englert, T. Wakita, and J. R. Wands.** 1996. Characterization of cell lines allowing tightly regulated expression of hepatitis C virus core protein. Virology **222:**51–63.

33. **Moriishi, K., T. Okabayashi, K. Nakai, K. Moriya, K. Koike, S. Murata, T. Chiba, K. Tanaka, R. Suzuki, T. Suzuki, T. Miyamura, and Y. Matsuura.** 2003. Proteasome activator PA28gamma-dependent nuclear retention and degradation of hepatitis C virus core protein. J. Virol. **77:**10237–10249.

34. **Moriya, K., H. Fujie, Y. Shintani, H. Yotsuyanagi, T. Tsutsumi, K. Ishibashi, Y. Matsuura, S. Kimura, T. Miyamura, and K. Koike.** 1998. The core protein of hepatitis C virus induces hepatocellular carcinoma in transgenic mice. Nat. Med. **4:**1065–1067.

35. **Moriya, K., K. Nakagawa, T. Santa, Y. Shintani, H. Fujie, H. Miyoshi, T. Tsutsumi, T. Miyazawa, K. Ishibashi, T. Horie, K. Imai, T. Todoroki, S. Kimura, and K. Koike.** 2001. Oxidative stress in the absence of inflammation in a mouse model for hepatitis C virus-associated hepatocarcinogenesis. Cancer Res. **61:**4365–4370.

36. **Moriya, K., H. Yotsuyanagi, Y. Shintani, H. Fujie, K. Ishibashi, Y. Matsuura, T. Miyamura, and K. Koike.** 1997. Hepatitis C virus core protein induces hepatic steatosis in transgenic mice. J. Gen. Virol. **78:**1527–1531.

37. **Neupert, W.** 1997. Protein import into mitochondria. Annu. Rev. Biochem. **66:**863–917.

38. **Okamoto, K., K. Moriishi, T. Miyamura, and Y. Matsuura.** 2004. Intramembrane proteolysis and endoplasmic reticulum retention of hepatitis C virus core protein. J. Virol. **78:**6370–6380.

39. **Okuda, M., K. Li, M. R. Beard, L. A. Showalter, F. Scholle, S. M. Lemon, and S. A. Weinman.** 2002. Mitochondrial injury, oxidative stress, and antioxidant gene expression are induced by hepatitis C virus core protein. Gastroenterology **122:**366–375.

40. **Perlemuter, G., A. Sabile, P. Letteron, G. Vona, A. Topilco, Y. Chretien, K. Koike, D. Pessayre, J. Chapman, G. Barba, and C. Bréchot.** 2002. Hepatitis C virus core protein inhibits microsomal triglyceride transfer protein activity and very low density lipoprotein secretion: a model of viral-related steatosis. FASEB J. **16:**185–194.

41. **Ralston, R., K. Thudium, K. Berger, C. Kuo, B. Gervase, J. Hall, M. Selby, G. Kuo, M. Houghton, and Q. L. Choo.** 1993. Characterization of hepatitis C virus envelope glycoprotein complexes expressed by recombinant vaccinia viruses. J. Virol. **67:**6753–6761.

42. **Ray, R. B., L. M. Lagging, K. Meyer, and R. Ray.** 1996. Hepatitis C virus core protein cooperates with ras and transforms primary rat embryo fibroblasts to tumorigenic phenotype. J. Virol. **70:**4438–4443.

43. **Roth, J., D. J. Taatjes, and M. J. Warhol.** 1989. Prevention of non-specific interactions of gold-labeled reagents on tissue sections. Histochemistry **92:**47–56.

44. **Sabile, A., G. Perlemuter, F. Bono, K. Kohara, F. Demaugre, M. Kohara, Y. Matsuura, T. Miyamura, C. Brechot, and G. Barba.** 1999. Hepatitis C virus core protein binds to apolipoprotein AII and its secretion is modulated by fibrates. Hepatology **30:**1064–1076.

45. **Santolini, E., G. Migliaccio, and N. La Monica.** 1994. Biosynthesis and biochemical properties of the hepatitis C virus core protein. J. Virol. **68:**3631–3641.

46. **Selby, M. J., Q. L. Choo, K. Berger, G. Kuo, E. Glazer, M. Eckart, C. Lee, D. Chien, C. Kuo, and M. Houghton.** 1993. Expression, identification and subcellular localization of the proteins encoded by the hepatitis C viral genome. J. Gen. Virol. **74:**1103–1113.

47. **Shimoike, T., S. Mimori, H. Tani, Y. Matsuura, and T. Miyamura.** 1999. Interaction of hepatitis C virus core protein with viral sense RNA and suppression of its translation. J. Virol. **73:**9718–9725.

48. **Suzuki, R., Y. Matsuura, T. Suzuki, A. Ando, J. Chiba, S. Harada, I. Saito, and T. Miyamura.** 1995. Nuclear localization of the truncated hepatitis C virus core protein with its hydrophobic C terminus deleted. J. Gen. Virol. **76:**53–61.

49. **Suzuki, R., K. Tamura, J. Li, K. Ishii, Y. Matsuura, T. Miyamura, and T. Suzuki.** 2001. Ubiquitin-mediated degradation of hepatitis C virus core protein is regulated by processing at its carboxyl terminus. Virology **280:**301–309.

50. **Tanaka, Y., T. Shimoike, K. Ishii, R. Suzuki, T. Suzuki, H. Ushijima, Y. Matsuura, and T. Miyamura.** 2000. Selective binding of hepatitis C virus core protein to synthetic oligonucleotides corresponding to the 5' untranslated region of the viral genome. Virology **270:**229–236.

51. **Tellinghuisen, T. L., and C. M. Rice.** 2002. Interaction between hepatitis C virus proteins and host cell factors. Curr. Opin. Microbiol. **5:**419–427.

52. **Thomson, M., and T. J. Liang.** 2000. Molecular biology of hepatitis C virus, p. 1–23. In T. J. Liang and J. H. Hoofnagle (ed.), Hepatitis C. Academic Press, San Diego, Calif.

53. **Weihofen, A., K. Binns, M. K. Lemberg, K. Ashman, and B. Martoglio.** 2002. Identification of signal peptide peptidase, a presenilin-type aspartic protease. Science **296:**2215–2218.

54. **Weis, K., I. W. Mattaj, and A. I. Lamond.** 1995. Identification of hSRP1 alpha as a functional receptor for nuclear localization sequences. Science **268:**1049–1053.

55. **Yanagi, M., R. H. Purcell, S. U. Emerson, and J. Bukh.** 1997. Transcripts from a single full-length cDNA clone of hepatitis C virus are infectious when directly transfected into the liver of a chimpanzee. Proc. Natl. Acad. Sci. USA **94:**8738–8743.

56. **Yasui, K., T. Wakita, K. Tsukiyama-Kohara, S. I. Funahashi, M. Ichikawa, T. Kajita, D. Moradpour, J. R. Wands, and M. Kohara.** 1998. The native form and maturation process of hepatitis C virus core protein. J. Virol. **72:**6048–6055.

ELSEVIER

Enhancement of mitochondrial gene expression in the liver of primary biliary cirrhosis

Cheng-Hsin Chen[a], Kazuyoshi Nagayama[a,c], Nobuyuki Enomoto[a,*], Yuka Miyasaka[a], Masayuki Kurosaki[a], Naoya Sakamoto[a], Shinya Maekawa[a], Sei Kakinuma[a], Takaaki Ikeda[d], Namiki Izumi[e], Chifumi Sato[b], Mamoru Watanabe[a]

[a] Department of Gastroenterology and Hepatology, Tokyo Medical and Dental University 1-5-45 Yushima, Bunkyo, Tokyo 113-8519, Japan
[b] Department of Health Science, Tokyo Medical and Dental University, 1-5-45 Yushima, Tokyo 113-8519, Japan
[c] Department of Internal Medicine, Tsuchiura Kyodo General Hospital 11-7 Manabe-Shinmachi, Tsuchiura, Ibaraki 300-0053, Japan
[d] Department of Internal Medicine, Yokosuka Kyosai General Hospital 22-7 Yonegahama-Dori, Yokosuka, Kanagawa 238-0011, Japan
[e] Department of Gastroenterology and Hepatology, Musashino Red Cross Hospital 1-26-1 Kyonan-cho, Musashino, Tokyo 180-8610, Japan

Abstract

Primary biliary cirrhosis (PBC) is one of the most important autoimmune liver diseases but the etiology and pathogenesis remain unknown. In this study, we analyzed differential mRNA expression in the liver of a patient with PBC using suppression subtractive hybridization to identify overexpressed genes. Overexpression of mRNA transcripts from mitochondrial DNA was observed in the PBC liver, compared to normal liver. To explore the mechanism of increased mitochondrial transcription, we investigated the mRNA levels of nuclear DNA-encoded regulator molecules of mitochondrial gene expression in 60 liver biopsy samples from various diseases, including PBC, using competitive RT-PCR. Increased expression of mitochondrial transcriptional factor A (mtTFA) and mitochondrial nuclear respiratory factor 1 (NRF-1) mRNA was demonstrated in PBC liver compared to other liver diseases, while NRF-1 coactivator 1, PGC-1 was suppressed. Mitochondrial DNA-encoded mRNA molecules are overexpressed in the PBC liver, and this is associated with up-regulation of mitochondrial transcription factor mtTFA and its transactivator NRF-1. Further studies are needed to focus on the relevance of this perturbation of mitochondrial gene expression in the pathogenesis of PBC.
© 2004 Elsevier B.V. All rights reserved.

Keywords: Suppression subtractive hybridization; Transcriptional factor; Reactive oxygen species

1. Introduction

Primary biliary cirrhosis (PBC) is a progressive autoimmune liver disease and currently, liver transplantation is the only lifesaving therapy for advanced disease [1]. While its etiologies remain unclear, they are thought to be due to immune-mediated or environmental [2], PBC is characterized by chronic progressive inflammatory destruction of in-

terlobular bile ducts. Anti-mitochondrial antibodies (AMA) are positive in most patients [3], and as a result of extensive investigations, their targets have been shown to be components of mitochondrial proteins, such as the E2 subunit of pyruvate decarboxylase (PDH-E2) [4,5]. However, the pathogenetic roles of the mitochondria themselves, as well as the autoimmune reaction directed to mitochondrial proteins, remain unknown.

Recently, several methods for comprehensive analysis of gene expression were developed and applied to a variety of diseases, e.g., serial analysis of gene expression (SAGE)

---

* Corresponding author. Tel.: +81 3 5803 5877; fax: +81 3 5803 0268.
E-mail address: enomoto@yamanashi.ac.jp (N. Enomoto).